Coherent effects on two-photon correlation and directional emission of two two-level atoms

C. H. Raymond Ooi,[1,2,*] Byung-Gyu Kim,[1] and Hai-Woong Lee[1]
[1]*Department of Physics, Korea Advanced Institute of Science and Technology, Daejeon, 305-701 Korea*
[2]*Max-Planck-Institut für Quantenoptik, D-85748, Garching, Germany*
(Received 27 February 2007; published 1 June 2007)

Sub- and superradiant dynamics of spontaneously decaying atoms are manifestations of collective many-body systems. We study the internal dynamics and the radiation properties of two atoms in free space. Interesting results are obtained when the atoms are separated by less than half a wavelength of the atomic transition, where the dipole-dipole interaction gives rise to new coherent effects, such as (a) coherence between two intermediate collective states, (b) oscillations in the two-photon correlation $G^{(2)}$, (c) emission of two photons by one atom, and (d) the loss of directional correlation. We compare the population dynamics during the two-photon emission process with the dynamics of single-photon emission in the cases of a Λ and a V scheme. We compute the temporal correlation and angular correlation of two successively emitted photons using the $G^{(2)}$ for different values of atomic separation. We find antibunching when the atomic separation is a quarter wavelength $\lambda/4$. Oscillations in the temporal correlation provide a useful feature for measuring subwavelength atomic separation. Strong directional correlation between two emitted photons is found for atomic separation larger than a wavelength. We also compare the directionality of a photon spontaneously emitted by the two atoms prepared in phased-symmetric and phased-antisymmetric entangled states $|\pm\rangle_{\mathbf{k}_0}=e^{i\mathbf{k}_0\cdot\mathbf{r}_1}|a_1,b_2\rangle\pm e^{i\mathbf{k}_0\cdot\mathbf{r}_2}|b_1,a_2\rangle$ by a laser pulse with wave vector $\mathbf{k}_0$. Photon emission is directionally suppressed along $\mathbf{k}_0$ for the phased-antisymmetric state. The directionality ceases for interatomic distances less than $\lambda/2$.

DOI: 10.1103/PhysRevA.75.063801 PACS number(s): 42.50.Fx, 42.50.Ar, 03.67.Mn

I. INTRODUCTION

Two atoms undergoing spontaneous emissions represent the simplest system for studying cooperative effects [1]. Recent advancements in cooling and trapping of atoms and ions provide the possibility of realizing such a system [2,3]. A trapped two-atom system is an efficient method for entangling atoms and photons, producing single-photon sources, and serving as two-qubit quantum gates [4], the basic building block for most quantum-computing schemes.

Although the two-atom system has been studied by many authors [5–10] in the past, certain aspects of the physics are still unexplored. Previous studies were based on the semiclassical theory and angular momentum basis [5,11]. The Dicke model disregards the position-dependent phase factor of each atom by assuming that the atomic separation is much smaller than a wavelength, $r/\lambda \ll 1$. Here, we do not make this approximation but use a full quantum treatment via the Schrödinger equation to calculate the transient dynamics of the two-atom system. In particular, when both atoms are within a wavelength distance, coherent effects give rise to interesting features in the properties of the emitted photons as well as the internal dynamics. Special attention is given to the directional emission of a photon emitted from collective states that are phased-symmetric and phased-antisymmetric entangled $|\pm\rangle_{\mathbf{k}_0}=e^{i\mathbf{k}_0\cdot\mathbf{r}_1}|a_1,b_2\rangle\pm e^{i\mathbf{k}_0\cdot\mathbf{r}_2}|b_1,a_2\rangle$ with a relative coherent phase, and quantum correlation between two successively emitted photons.

In Sec. II we present the Schrödinger approach to the problem. We compare the dynamics of the populations in $|\pm\rangle$ for the Λ, $\diamond$, and V schemes for two mutually orthogonal transitions ($\sigma^{\pm}$ and π) and scalar photons, which provides intuitive understanding. The results for the V scheme are used in Sect. III to study the directional properties of the spontaneously emitted photon. Contrasting directional correlations are found for atoms prepared initially in phased-symmetric and phased-antisymmetric entangled states by excitation of a laser pulse. In Sec. IV, we compute Glauber's two-photon correlation $G^{(2)}$ and show how the vacuum-induced dipole-dipole coupling gives an oscillatory feature as a function of τ (delay in detection time) that provides a potentiality for subwavelength resolution. We also compute $G^{(2)}$ as a function of the angle between two detectors to analyze the angular correlation between the two successively emitted photons.

II. COLLECTIVE DYNAMICS

The full atom-radiation dynamics of the two-atom system in free space [Fig. 1(a)] can be studied starting from the interaction Hamiltonian

$$V(t)=-\sum_{j=1,2}\sum_{\mathbf{k}}\hbar\{g_{\mathbf{k}}^{j}\hat{a}_{\mathbf{k}}|a_j\rangle\langle b_j|e^{i\mathbf{k}\cdot\mathbf{r}_j}e^{-i\Delta_{\mathbf{k}}t}+\text{adj}\} \qquad (1)$$

where $g_{\mathbf{k}}^{(j)}=\vec{\wp}^{(j)}\cdot\hat{\varepsilon}_{\mathbf{k}}\sqrt{\nu_{\mathbf{k}}/2\varepsilon_0\hbar V}$ is the free space coupling coefficient for the jth atom. The quantum dynamics of the two-atom system and the properties of emitted photon(s) depend on the initial states and the scheme. Below, we present the dynamics of three possible schemes with different initial states for two atoms interacting with radiation in free space.

A. Initial $|a_1,a_2,0\rangle$, final $|b_1,b_2,1_{\mathbf{k}},1_{\mathbf{q}}\rangle$ ($\diamond$ scheme)

Here, we consider the full four-state scheme in Fig. 1(c), where the presence of a second photon $\mathbf{q}$ makes it different

*Email address: bokooi73@yahoo.com

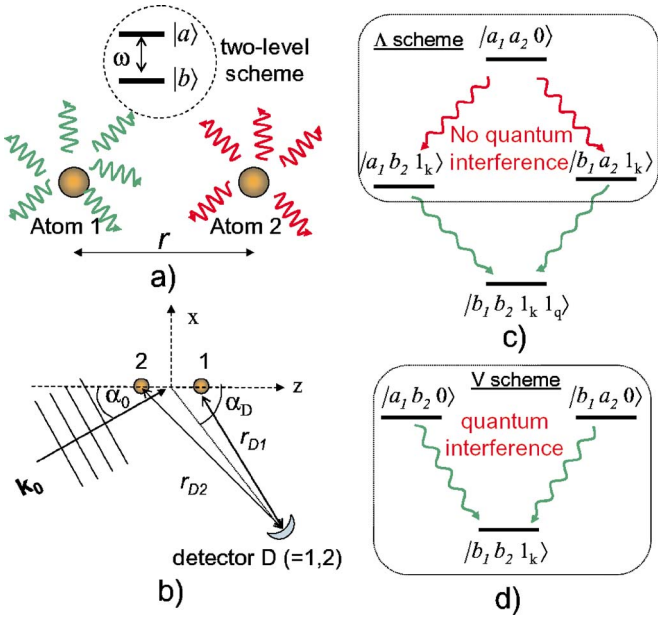

FIG. 1. (Color online) (a) Two particles (atoms), each with two levels separated by a distance r. In practice, the particles could be atoms or ions in a trap. (b) Timed excitation [12] using a laser with wave vector $\mathbf{k}_0$ and detection by detector D $(=A,B)$ for the intensity distribution $I(\alpha,r)$ or two-photon correlation $G^{(2)}(\alpha_A,\alpha_B,r,\tau)$ using two detectors. (c) Double cascade (or $\diamond$ scheme) composite four basis states for two-atom radiation system. If the ground state is neglected, we have the Λ scheme with no Fano interference. (d) V scheme: The system can start from an entangled state composed of a superposition of the intermediate states with no photon and decay to the ground state, giving Fano interference.

from the Λ scheme to be considered in Sec. II B. The atoms are initially in the excited state with radiation in the vacuum, i.e., $|a_1,a_2,0\rangle$ with $|0\rangle$ as the vacuum state. One of the atoms may then decay to either state $|b_1,a_2,1_\mathbf{k}\rangle$ or $|a_1,b_2,1_\mathbf{k}\rangle$ with the emission of a photon $\mathbf{k}$. Subsequently, another atom decays to the final state $|b_1,b_2,1_\mathbf{k},1_\mathbf{q}\rangle$, emitting a photon $\mathbf{q}$.

The radiation-system state vector can be written as a superposition of the atoms field collective basis [Fig. 1(c)],

$$|\Psi(t)\rangle = A(t)|a_1,a_2,0\rangle + \sum_{\mathbf{k},\mathbf{q}} C_{\mathbf{kq}}(t)|b_1,b_2,1_\mathbf{k},1_\mathbf{q}\rangle + \sum_{\mathbf{k}} [B_\mathbf{k}^{(1)}(t)|b_1,a_2,1_\mathbf{k}\rangle + B_\mathbf{k}^{(2)}(t)|a_1,b_2,1_\mathbf{k}\rangle]. \quad (2)$$

Note that the state Eq. (2) can be rewritten as the product state for two atoms, $|\Psi(t)\rangle=\Pi_{j=1,2}[\beta^{(j)}(t)|a_j,0\rangle + \Sigma_\mathbf{k}\gamma_\mathbf{k}^{(j)}(t)|b_j,1_\mathbf{k}\rangle]$. The coupled equations for the coefficients in Eq. (2) are given in Appendix A. We proceed to obtain the transient solutions for the coefficients.

1. Excited-state dynamics

The excited-state coefficient decays exponentially with the total rate of the two atoms,

$$A(t) = A(0)e^{-(\Gamma^{(1)}+\Gamma^{(2)})t/2}. \quad (3)$$

2. Symmetric and antisymmetric state dynamics

In the following, we assume that the two atoms are identical, $\Gamma^{(1)}=\Gamma^{(2)}$. By defining $\tilde{B}_\mathbf{k}^{(\pm)}(t)=(1/\sqrt{2})[\tilde{B}_\mathbf{k}^{(1)}(t)\pm\tilde{B}_\mathbf{k}^{(2)}(t)]$ as the coefficients for the symmetric and antisymmetric entangled states $|\pm\rangle=(1/\sqrt{2})(|a_1,b_2,1_\mathbf{k}\rangle\pm|b_1,a_2,1_\mathbf{k}\rangle)$, we can write the transient solutions in a much simpler form than $\tilde{B}_\mathbf{k}^{(j)}(t)$ for the individual states $|a_i,b_j,1_\mathbf{k}\rangle$. For the initial conditions $B_\mathbf{k}^{(j)}(0)=0$ and $A(0)=1$, we have

$$\tilde{B}_\mathbf{k}^{(\pm)}(t) = i\frac{A(0)}{\sqrt{2}}e^{-\Gamma t}g_\mathbf{k}^{(\pm)*}\frac{1-e^{-(i\Delta_\mathbf{k}-\tilde{\Gamma}^{(\mp)}/2)t}}{i\Delta_\mathbf{k}-\frac{1}{2}\tilde{\Gamma}^{(\mp)}}, \quad (4)$$

where the symmetric and antisymmetric coupling coefficients and the complex rates which depend on atomic positions are, respectively,

$$g_\mathbf{k}^{(\pm)} = g_\mathbf{k}^{(1)}e^{i\mathbf{k}\cdot\mathbf{r}_1}\pm g_\mathbf{k}^{(2)}e^{i\mathbf{k}\cdot\mathbf{r}_2}, \quad (5)$$

$$\tilde{\Gamma}^{(\pm)} = \Gamma \pm \eta\Gamma f(r) = \Gamma^{(\pm)} \pm i\eta\Gamma h(r), \quad (6)$$

where $\Gamma^{(\pm)}\doteq\Gamma[1\pm\eta g(r)]$ is the superradiant $(+)$ and subradiant rate $(-)$, respectively, and $\eta\doteq\sqrt{\hat{\wp}^{(2)*}\cdot\hat{\wp}^{(1)}/\hat{\wp}^{(1)*}\cdot\hat{\wp}^{(2)}}$. The dependency on the atomic separation r enters through

$$f(r) = g(r) + ih(r), \quad (7)$$

with $g(r)$ modifying the decay rate and $h(k_0r)$ giving the energy level shift and dipole-dipole interaction, whose expressions are given in Appendix B for scalar and vector photons from π and $\sigma^\pm$ transitions. Note that these are collective effects due to indirect interaction between the two atoms as induced by the vacuum field since the atoms have no permanent dipoles.

By paying attention to the level shift $\frac{1}{2}\Gamma h(r)$ due to dipole-dipole interaction, the coefficients $\tilde{B}_\mathbf{k}^{(\pm)}$ should be redefined as

$$\mathcal{B}_\mathbf{k}^{(\pm)}(t) = B_\mathbf{k}^{(\pm)}(t)e^{\pm i\Gamma ht/2} = \tilde{B}_\mathbf{k}^{(\pm)}(t)e^{i\Delta_\mathbf{k}^\pm t} \quad (8)$$

where $\Delta_\mathbf{k}^\pm=\Delta_\mathbf{k}\pm\frac{1}{2}\Gamma h=\nu_\mathbf{k}-\omega^\mp$, $\omega^\mp(r)=\omega\mp\frac{1}{2}\Gamma h(r)$ is the shifted atomic transition frequency, and $B_\mathbf{k}^{(\pm)}=(1/\sqrt{2})\times(B_\mathbf{k}^{(1)}\pm B_\mathbf{k}^{(2)})$.

For the purpose of comparing with the collective Λ scheme for single-photon emission of Fig. 1(c), we express Eq. (4) in a more intuitive form,

$$\mathcal{B}_\mathbf{k}^{(\pm)}(t) = -i\frac{A(0)}{\sqrt{2}}g_\mathbf{k}^{(\pm)*}\frac{e^{-\Gamma^{(\pm)}t/2}-e^{i\Delta_\mathbf{k}^\pm t}e^{-\Gamma t}}{i\Delta_\mathbf{k}^\pm-\frac{1}{2}\Gamma^{(\mp)}}. \quad (9)$$

By comparing Eq. (9) (for the double-cascade scheme) with Eq. (18) (for the Λ scheme), we see that the symmetric and antisymmetric states have different r-dependent linewidths $\frac{1}{2}\Gamma^{(\pm)}(r)$ or transition rates, and modified transition energies $\omega^\pm=\omega\pm\frac{1}{2}\Gamma h(r)$ due to the dipole-dipole interaction and the presence of the fourth state, the ground state $|b_1,b_2\rangle$.

The populations in states $|\pm\rangle$ can be obtained from $P^{(\pm)}(t)=\Sigma_\mathbf{k}|\tilde{B}_\mathbf{k}^{(\pm)}(t)|^2$ as

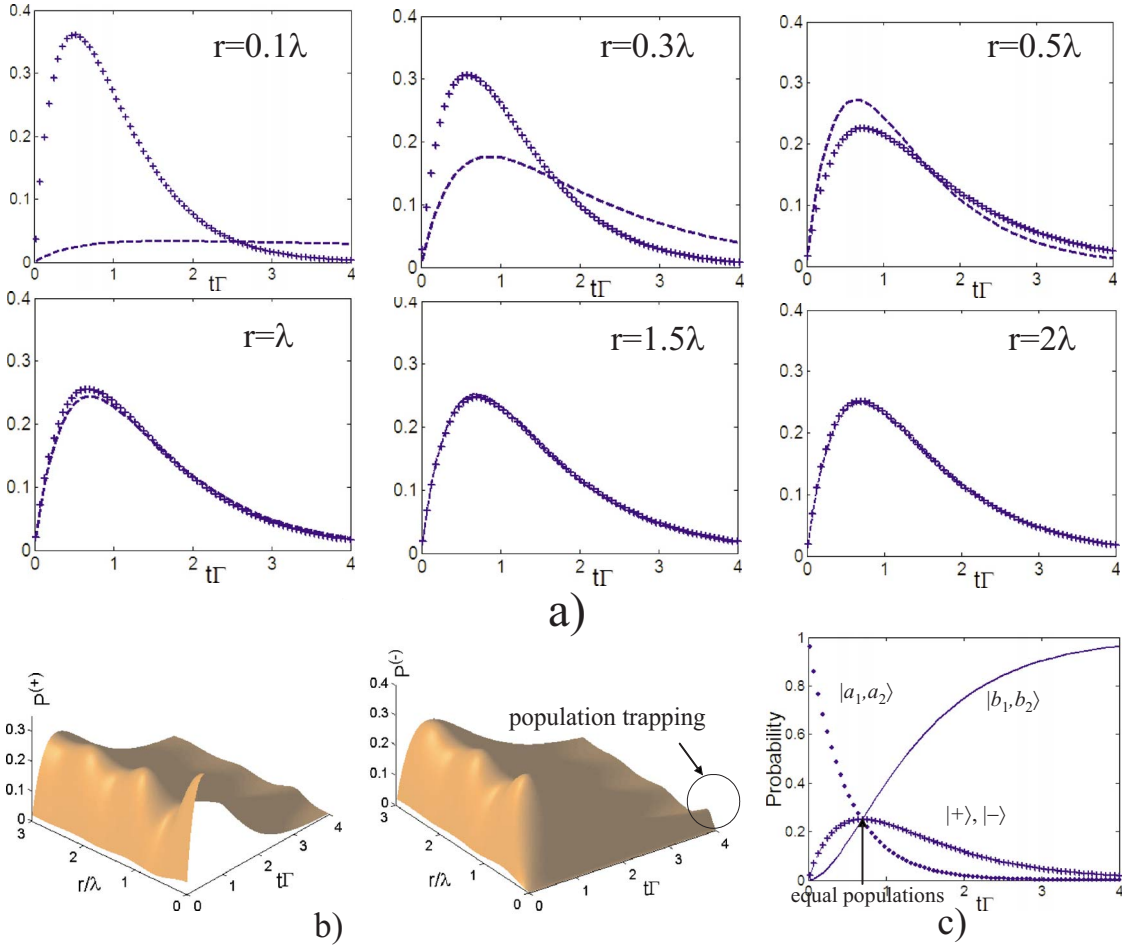

FIG. 2. (Color online) Transient dynamics for the full four-level scheme for $\Delta M=\pm 1$ transitions. (a) Populations $P^{(\pm)}$ in $|\pm\rangle=(1/\sqrt{2})(|a_1,b_2\rangle\pm|b_1,a_2\rangle)|1_{\mathbf{k}}\rangle$ versus time for different interatomic distances. The populations increase rapidly at small times, reach a maximum at around $3/(4\Gamma)$, and fall off gradually. A subtle feature is that at large r the peaks of the two states oscillate closely around 0.25, the value at large interatomic distance. Note that the peak for $P^{(-)}$ $(----)$ is lower than the peak for $P^{(+)}$ $(++++)$ when $r=n\lambda$ with n being an integer. (b) Three-dimensional (3D) plots of $P^{(\pm)}$ show additional features. The two populations are different in the region $r\lesssim\lambda$. At $r\simeq\lambda/4$ the population in state $|-\rangle$ is not depleted even at large times. (c) Transient populations for all states in the large-r limit. The populations are the same around time $3/(4\Gamma)$

.

$$P^{(\pm)}\simeq\frac{\Gamma}{\Gamma^{(\mp)}}(e^{\Gamma^{(\pm)}t}-e^{-2\Gamma t})\left[1\pm\frac{\eta+\eta^*}{2}\left(\frac{\omega^{\mp}}{\omega}\right)^3 g(r)^{\mp}\right], \tag{10}$$

where $g(r)^{\mp}=g(r)_{\omega\to\omega^{\mp}}$. For $\eta=1$ and $\omega^{\mp}\simeq\omega$, we find

$$P^{(\pm)}\simeq(e^{-\Gamma^{(\pm)}t}-e^{-2\Gamma t})\frac{1\pm g(r)}{1\mp g(r)}. \tag{11}$$

At time $t=0$ we verify that $P^{(\pm)}(0)=0$. In the limit $r\to\infty$ we have $g(r)\to 0$ and $P^{(\pm)}\to e^{-2\Gamma t}(e^{\Gamma t}-1)$. Moreover, Fig. 2 shows that the peaks of the populations for large r are equal, i.e., 0.25. When $r\to 0$ we have $g(r)\to 1$. By defining $1-g(r)=\delta$ we obtain $P^{(+)}(r\to 0)\simeq(2/\delta)e^{-2\Gamma t}(e^{\delta\Gamma t}-1)\simeq 2\Gamma t e^{-2\Gamma t}$ and $P^{(-)}(r\to 0)\to 0$. Thus, in the limit of very small interatomic distance, only the symmetric state is occupied, and its population increases linearly with time in the beginning and then falls off exponentially. The antisymmetric state is essentially unoccupied. In Appendix E, we show that there is no coherence between the symmetric and antisymmetric states even for small r, i.e., $\rho_{-+}(t)=0$.

3. Coherence

Note that the four-state scheme is identical to the double-cascade scheme [13]. We might wonder about the connection between the collective effects and spontaneously generated coherence.

From the result in Appendix E and using $\rho_{-+}\doteq\langle-|\hat{\rho}(t)|+\rangle=\frac{1}{2}(\rho_{11}-\rho_{22}+\rho_{12}-\rho_{21})$ where $|1\rangle\doteq|a_1,b_2,1_{\mathbf{k}}\rangle$ and $|2\rangle\doteq|a_2,b_1,1_{\mathbf{k}}\rangle$, we find

$$(\rho_{12}-\rho_{21})=\rho_{22}-\rho_{11}. \tag{12}$$

Equation (12) indicates that there is a finite coherence between $|a_1,b_2,1_{\mathbf{k}}\rangle$ and $|a_2,b_1,1_{\mathbf{k}}\rangle$ when their populations are

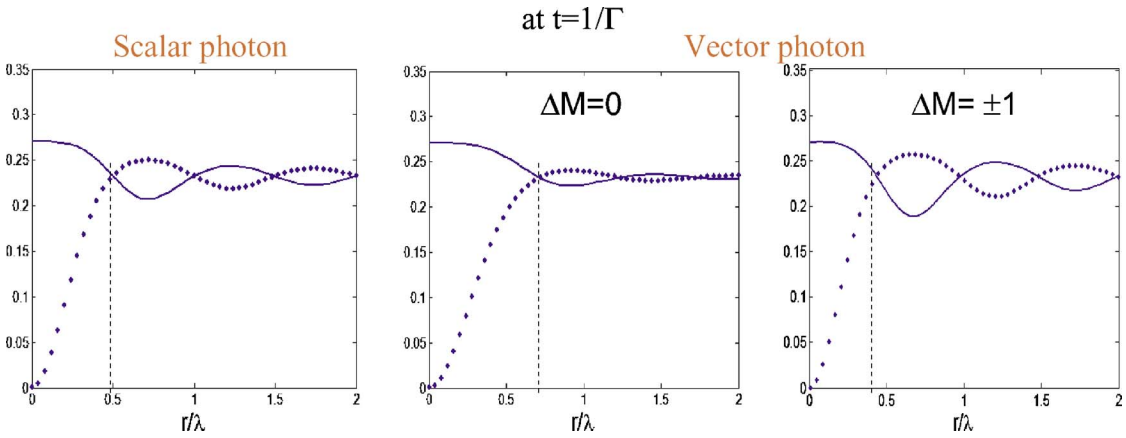

FIG. 3. (Color online) Comparison of the populations in the bright state $P^{(+)}$ (solid line) and the dark state $P^{(-)}$ (dots) for the scalar photon with $g=(\sin kr)/kr$ and the vector photon with $g^{\parallel}=[3/(kr)^3](\sin kr-kr\cos kr)$ for linear polarization or $\Delta M=0$ and $g^{\perp}=\frac{3}{2}[(\sin kr)/kr+(\cos kr)/(kr)^2-(\sin kr)/(kr)^3]$ for circular polarization or $\Delta M=\pm 1$. The result with the scalar photon gives physical insight but the results with the vector photon do not, since the nodes do not fall exactly at $n\lambda/2$.

not equal. This occurs obviously for $r \lesssim \lambda/2$ where the collective effects are significant as clearly shown in Figs. 2(a) and 3. Thus, the coherence must have been induced by the dipole-dipole interaction, much like the spontaneously generated coherence in the double-cascade or $\diamondsuit$ scheme.

4. Photon trapping

The above results are entirely different from those for the Λ scheme in Sec II B where the ground state $|b_1,b_2\rangle$ is excluded. For small atomic separations, the long tail in Figs. 2(a) and 2(b) shows a slow-decaying dynamics for the antisymmetric state $|-\rangle$ as pointed out earlier by Stephen [6]. The state is also a dark state in the sense that it is weakly populated from $|a_1,a_2,0\rangle$, as shown in Fig. 2(a). This so-called subradiant or trapping state is the result of coherent population trapping where the coherence between $|a_1,b_2,1_{\mathbf{k}}\rangle$ and $|b_1,a_2,1_{\mathbf{k}}\rangle$ (as shown in Sec. II A 3) introduces repeated emissions and reabsorptions of photons, which manifests itself as coherence-induced photon trapping [5] between the two atoms, which act like cavity mirrors. This coherent phenomenon can also be understood via the concept of phase locking [14].

5. Ground-state dynamics

The transient solution as found from Eq. (A4) is

$$C_{\mathbf{kq}}(t) = -\frac{A(0)}{2} g_{\mathbf{q}}^* g_{\mathbf{k}}^* \left[\frac{G_{\mathbf{kq}}^+}{\frac{1}{2}\tilde{\Gamma}^{(-)} - i\Delta_{\mathbf{k}}} \left(\frac{1-e^{-(\Gamma^{(+)}/2 - i\Delta_{\mathbf{q}})t}}{\frac{1}{2}\tilde{\Gamma}^{(+)} - i\Delta_{\mathbf{q}}} - \frac{1-e^{-(\Gamma - i\Delta_{\mathbf{k}} - i\Delta_{\mathbf{q}})t}}{\Gamma - i\Delta_{\mathbf{k}} - i\Delta_{\mathbf{q}}} \right) + \frac{G_{\mathbf{kq}}^-}{\frac{1}{2}\tilde{\Gamma}^{(+)} - i\Delta_{\mathbf{k}}} \left(\frac{1-e^{-(\Gamma^{(-)}/2 - i\Delta_{\mathbf{q}})t}}{\frac{1}{2}\tilde{\Gamma}^{(-)} - i\Delta_{\mathbf{q}}} - \frac{1-e^{-(\Gamma - i\Delta_{\mathbf{k}} - i\Delta_{\mathbf{q}})t}}{\Gamma - i\Delta_{\mathbf{k}} - i\Delta_{\mathbf{q}}} \right) + (\mathbf{k} \leftrightarrow \mathbf{q}) \right], \tag{13}$$

where

$$G_{\mathbf{kq}}^{\pm} = \{ e^{-i\mathbf{q}\cdot\mathbf{r}_1} e^{-i\mathbf{k}\cdot\mathbf{r}_2} + e^{-i\mathbf{q}\cdot\mathbf{r}_2} e^{-i\mathbf{k}\cdot\mathbf{r}_1} \pm e^{-i(\mathbf{k}+\mathbf{q})\cdot\mathbf{r}_1} \pm e^{-i(\mathbf{k}+\mathbf{q})\cdot\mathbf{r}_2} \}. \tag{14}$$

The steady-state solution follows from Eq. (13) as

$$C_{\mathbf{kq}}(\infty) = -\frac{1}{2} A(0) g_{\mathbf{q}}^* g_{\mathbf{k}}^* \frac{1}{\Gamma - i\Delta_{\mathbf{k}} - i\Delta_{\mathbf{q}}} \left[\left(\frac{G_{\mathbf{kq}}^+}{\left(\frac{1}{2}\Gamma^{(+)} - i\Delta_{\mathbf{k}}\right)} + \frac{G_{\mathbf{kq}}^-}{\left(\frac{1}{2}\Gamma^{(-)} - i\Delta_{\mathbf{k}}\right)} \right) + (\mathbf{k} \leftrightarrow \mathbf{q}) \right]. \tag{15}$$

Note that Eq. (15) corresponds to the *superposition of two cascade transitions* (via states $|+\rangle$ and $|-\rangle$) as in Sec. 6.4 of [15]. The denominator $\Gamma - i\Delta_{\mathbf{k}} - i\Delta_{\mathbf{q}}$ shows that the $\mathbf{k}$ and $\mathbf{q}$ photons are correlated. The term $\Sigma_{j=1,2} e^{-i(\mathbf{k}+\mathbf{q})\cdot\mathbf{r}_j}$ gives the *directional correlation* between the $\mathbf{k}$ and $\mathbf{q}$ photons as it reduces to a δ function for a large number of atoms.

The populations in the ground state $|b_1, b_2, 1_{\mathbf{k}}, 1_{\mathbf{q}}\rangle$ can be calculated indirectly from

$$P_{b_1,b_2}(t) = \sum_{\mathbf{k},\mathbf{q}} |C_{\mathbf{kq}}(t)|^2 = 1 - e^{-2\Gamma t} - \sum_{\mathbf{k},j=1,2} |\tilde{B}_{\mathbf{k}}^{(j)}(t)|^2. \tag{16}$$

This avoids the complication of evaluating $\Sigma_{\mathbf{k},\mathbf{q}}|C_{\mathbf{kq}}(t)|^2$. We plot Eq. (16) in Fig. 2(c). In the limit $r \to \infty$ we find $P_{b_1,b_2} \to 1 - e^{-\Gamma t}$.

6. Scalar photon vs vector photon

Here, we compare the probabilities between the scalar and vector photons at a fixed time, say $t = 1/\Gamma$. The distinction between scalar and vector photons comes from the $g(r)$ and $h(r)$ functions defined in Appendix B. The scalar photon assumes that the photon is emitted only along the interatomic axis, i.e., the z axis. Thus, $\theta = 0$ gives $\mathbf{k} = \hat{z}k$, with the two polarizations $\hat{\varepsilon}_{\mathbf{k}1} = (\cos\varphi, \sin\varphi, 0)$, $\hat{\varepsilon}_{\mathbf{k}2} = (-\sin\varphi, \cos\varphi, 0)$. Then $\Sigma_{\lambda=1,2} \epsilon_{\mathbf{k}\lambda p} \epsilon^*_{\mathbf{k}\lambda p} = 1$, where $p = x, y$.

At a fixed time, Fig. 3 shows that $P^{\pm}$ oscillate with interatomic distance. The scalar photon model [Fig. 3(a)] shows that for integrals of the half wavelength, i.e., $n\lambda/2$, the populations are equal, $P^+ = P^-$. This simple model gives an intuitive physical interpretation. The emitted photon forms a standing wave between the two atoms. The atoms on the nodes essentially do not experience the presence of the photon field and hence the effect of the neighboring atom. For distances below $\lambda/2$, the probability of emitting a photon and going into $|-\rangle$ becomes exceedingly small. Here, we note that the two atoms in state $|-\rangle$ act like a subwavelength cavity where spontaneous emission is inhibited [16]. By comparing Figs. 4 and 3, we see that the emission of the second photon to the state $|b_1, b_2, 1_k, 1_q\rangle$ causes the total population $P^{(+)} + P^{(-)}$ to decrease for $r < \lambda/2$. Also, the first node for $\Delta M = 0$ is greater than $\lambda/2$, while the first node for $\Delta M = \pm 1$ is smaller than $\lambda/2$.

B. Initial $|a_1, a_2, 0\rangle$, final $|\pm\rangle$ (Λ scheme)

When the decay to the ground state $|b_1, b_2\rangle$ can be neglected or suppressed, the two-atom system can be modeled as a Λ scheme, as depicted in Fig. 1(c). The purpose of discussing this scheme is for comparison with the full four-state scheme.

The atoms are initially in $|a_1, a_2, 0\rangle$ and decay to the maximally entangled symmetric $(+)$ or antisymmetric $(-)$ states $|\pm\rangle = (1/\sqrt{2})(|a_1, b_2\rangle \pm |b_1, a_2\rangle)|1_{\mathbf{k}}\rangle$ with the emission of photon $\mathbf{k}$. As shown in Appendix C, the excited-state dynamics is independent of the interatomic separation and decays exponentially as

$$A(t) = A(0)e^{-Gt}, \tag{17}$$

where $G = \Gamma^{(1)} + \Gamma^{(2)}$, while the $|\pm\rangle$ states are governed by

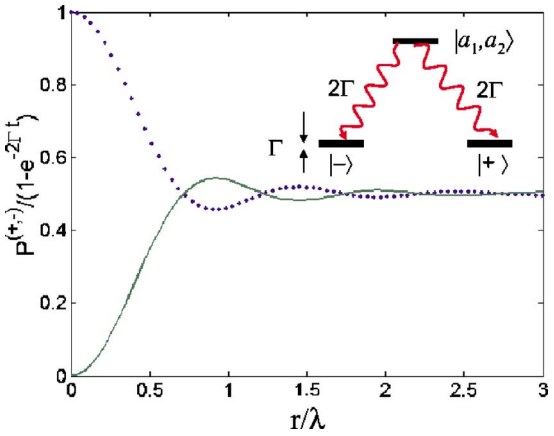

FIG. 4. (Color online) Probabilities $P^{(\pm)}$ [Eq. (19)] in the bright state $|+\rangle$ (dots) and dark state $|-\rangle$ (line) for a three-state system [inset of Fig. 1(c)], where the decay to state $|b_1, b_2, 1_k, 1_q\rangle$ is not considered or neglected and $|\pm\rangle = (1/\sqrt{2})(|a_1, b_2\rangle \pm |b_1, a_2\rangle)|1_{\mathbf{k}}\rangle$. We use the $\Delta M = 0$ transition.

$$B_{\mathbf{k}}^{(\pm)}(t) = -\frac{A(0)}{\sqrt{2}} \frac{1 - e^{(i\Delta_{\mathbf{k}} - G)t}}{\Delta_{\mathbf{k}} + iG} (g_{\mathbf{k}}^{(2)*} \pm g_{\mathbf{k}}^{(1)*}) \tag{18}$$

with probabilities

$$P^{(\pm)}(t) = \frac{1}{2}(1 - e^{-2Gt}) \left(1 \pm \frac{2\sqrt{\Gamma^{(1)}\Gamma^{(2)}}}{\Gamma^{(1)} + \Gamma^{(2)}} g(r)\right)$$

$$\simeq \frac{1}{2}(1 - e^{-2\Gamma t})[1 \pm g(r)], \tag{19}$$

where we assume $\Gamma^{(1)} \simeq \Gamma^{(2)}$, with the $g(r)$ and $h(r)$ functions defined in Ref. [10] and produced in Appendix B. The correctness of Eq. (19) is verified since $|A|^2 + \Sigma_{\mathbf{k},j=1,2}|B_{\mathbf{k}}^{(j)}|^2 = |A|^2 + \Sigma_{\mathbf{k}}[|B_{\mathbf{k}}^{(+)}(t)|^2 + |B_{\mathbf{k}}^{(-)}(t)|^2] = e^{-2\Gamma t} + (P^{(+)} + P^{(-)}) = 1$.

The dynamics of $P^{(\pm)}(t)$ are plotted in Fig. 4. Here, the populations in $|+\rangle$ and $|-\rangle$ are substantially different for small r. But the transient dynamics of $|+\rangle$ and $|-\rangle$ are the same, governed by the rate 2Γ. For initial coherent excitation $A(0) = e^{i\mathbf{k}_0\cdot(\mathbf{r}_1 + \mathbf{r}_2)}$ we obtain (see Appendix C) the single-photon amplitude $\Psi^{(1)}(\mathbf{r}_D, t_D)$, defined as

$$\langle 0|\hat{E}(\mathbf{r}_D, t_D)|\Psi(\infty)\rangle = i\frac{1}{2}\frac{\wp^* \omega^3 e^{i\mathbf{k}_0\cdot(\mathbf{r}_1 + \mathbf{r}_2)}}{3\pi\varepsilon_0 c^3} \times \sum_{j=1,2} A_j e^{-(i\omega + G)\tau_{Dj}} \Theta(\tau_{Dj}) \tag{20}$$

where $\tau_{Dj} = t_D - r_{Dj}/c$ and A_j are defined by Eqs. (C9). The intensity goes as $|A_1|^2 + |A_2|^2 + A_1 A_2^* e^{-G(\tau_{D1} + \tau_{D2})} e^{i\omega(\tau_{D2} - \tau_{D1})}$ + c.c., and there is no preference in the direction.

C. Initial entangled states (V scheme)

Now, we consider the case where the initial state is

$$|\Psi(0)\rangle = [B^{(2)}(0)|a_1, b_2\rangle + B^{(1)}(0)|b_1, a_2\rangle]|0\rangle \tag{21}$$

where $|B^{(2)}(0)|^2 + |B^{(2)}(0)|^2 = 1$ for $C_{\mathbf{k}}(0) = 0$. The fact that this state has no photon makes it different from the intermediate

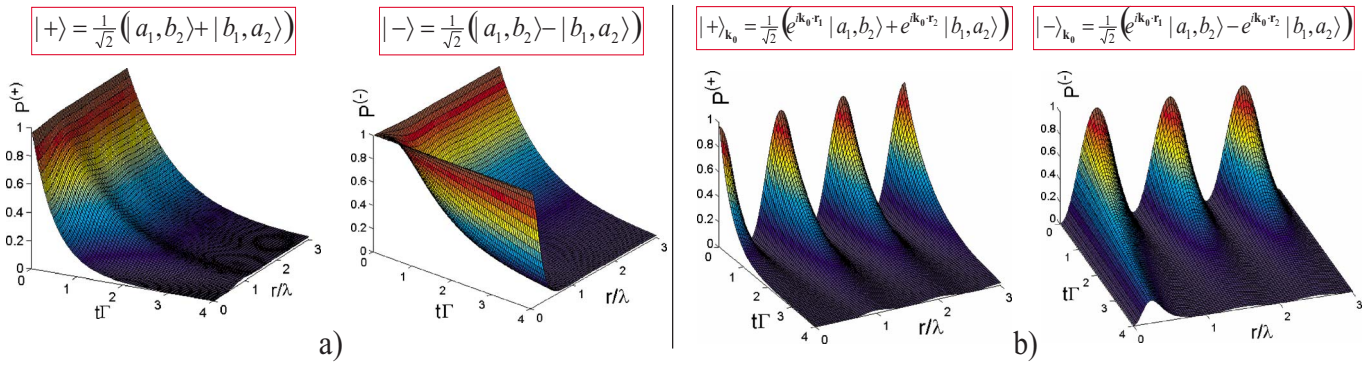

FIG. 5. (Color online) Populations $P^{(\pm)}$ in the bright or symmetric entangled state $|+\rangle$ and the dark or antisymmetric entangled state $|-\rangle$ state for V scheme computed from Eq. (23) for $\Delta M=0$ transition. For $r \ll \lambda$, the $|+\rangle$ state decays at a superradiant rate, and the $|-\rangle$ state decays at a subradiant rate. The inset shows the V scheme with the collective states. (b) The populations computed using Eq. (25) for initial phased-entangled states $|\pm\rangle_{\mathbf{k}_0}=(1/\sqrt{2})(e^{i\mathbf{k}_0\cdot\mathbf{r}_1}|a_1,b_2\rangle \pm e^{i\mathbf{k}_0\cdot\mathbf{r}_2}|a_2,b_1\rangle)$ prepared by timed excitation with a laser pulse incident at an angle α_0. We have used $\alpha_0=0°$, which gives a maximum phase difference between the two atoms. The oscillations are due to the finite phase difference. Note that $\alpha_0=90°$, which corresponds to no phase difference gives the results in (a).

states of Sec. II A. The state decays to $|b_1,b_2,1_{\mathbf{k}}\rangle$ and the collective system can be represented by a three-level V scheme [Fig. 1(d)]. The detailed calculations of the decay dynamics are given in Appendix D.

For $\Gamma^{(1)}=\Gamma^{(2)}$ we have

$$B^{(\pm)}(t) = e^{-\tilde{\Gamma}^{(\pm)}t/2}B^{(\pm)}(0), \tag{22}$$

where $B^{(\pm)}(t)=(1/\sqrt{2})[B^{(1)}(t)\pm B^{(2)}(t)]$ are the coefficients for the $|\pm\rangle$ states. The probabilities

$$P^{(\pm)}(t) = e^{-\tilde{\Gamma}^{(\pm)}t}|B^{(\pm)}(0)|^2 \tag{23}$$

are plotted in Fig. 5(a) for the initial symmetric $[B^{(+)}(0)=1, B^{(-)}(0)=0]$ and antisymmetric $[B^{(-)}(0)=1, B^{(+)}(0)=0]$ entangled states $|\pm\rangle=(1/\sqrt{2})(|a_1,b_2\rangle \pm |b_1,a_2\rangle)|0\rangle$, which correspond to the superradiant and subradiant states, respectively. The transient dynamics of $|\pm\rangle$ are correlated with r for the V scheme as seen from Eq. (22) but not for the Λ scheme. The two states are depleted at different rates that depend on r.

If the atoms are prepared in an entangled state upon single-photon absorption by a laser pulse with a wave vector $\mathbf{k}_0$ [12], we can choose $B^{(2)}_{\mathbf{k}}(0)=\sqrt{p}e^{i\mathbf{k}_0\cdot\mathbf{r}_1}$ and $B^{(1)}(0)=\sqrt{1-p}e^{i\mathbf{k}_0\cdot\mathbf{r}_2}$ and have the initial states

$$|\pm\rangle^p_{\mathbf{k}_0} = (\sqrt{p}e^{i\mathbf{k}_0\cdot\mathbf{r}_1}|a_1,b_2\rangle \pm \sqrt{1-p}e^{i\mathbf{k}_0\cdot\mathbf{r}_2}|b_1,a_2\rangle)|0\rangle \tag{24}$$

with $0\leq p\leq 1$.

For $p=1/2$, the states (referred simply as $|\pm\rangle_{\mathbf{k}_0}$) are maximally entangled, and they are orthogonal $({}_{\mathbf{k}_0}\langle -|+\rangle_{\mathbf{k}_0}=0)$ or mutually exclusive. In other words, one cannot derive the properties of state $|-\rangle_{\mathbf{k}_0}$ from the properties of state $|+\rangle_{\mathbf{k}_0}$. This is clearly seen in Figs. 6 and 7. The states $|-\rangle_{\mathbf{k}_0}$ and $|+\rangle_{\mathbf{k}_0}$ are related only for certain sets of atomic positions [17].

The state Eq. (24) gives $|B^{(\pm)p}(0)|^2=\frac{1}{2}[1\pm 2\sqrt{p(1-p)}\cos\mathbf{k}_0\cdot\mathbf{r}_{12}]$ and hence probabilities that further depend on r and α_0 [see Fig. 1(b)]

$$P^{(\pm)p}(t) = e^{-\tilde{\Gamma}^{(\pm)}t}\frac{1}{2}[1\pm 2\sqrt{p(1-p)}\cos(\mathbf{k}_0\cdot\mathbf{r}_{12})], \tag{25}$$

where the visibility of the interference is maximum when $p=1/2$. The wave vector $\mathbf{k}_0$ provides a relative phase between the two atoms that depend on their separation. The maximally entangled states $|\pm\rangle_{\mathbf{k}_0}$ are the two extremes that would give more interesting results than the nonmaximally entangled states; thus we take $p=1/2$ from here.

Again, if the atoms are initially prepared in the state $|\pm\rangle_{\mathbf{k}_0}$ by the wave vector $\mathbf{k}_0$, the steady-state coefficient for the ground state $|b_1,b_2,1_{\mathbf{k}}\rangle$ can be written as

$$C_{\mathbf{k}}(\infty)_{|\pm\rangle_{\mathbf{k}_0}} = \frac{-ig^*_{\mathbf{k}}}{\sqrt{2}2x_{12}}\left(\frac{1}{(a_+ - i\Delta_{\mathbf{k}})} - \frac{1}{(a_- - i\Delta_{\mathbf{k}})}\right) \times\left[\left(\frac{1}{2}\Gamma - i\Delta_{\mathbf{k}}\right)\sum_{j=1,2} e^{-i(\mathbf{k}-\mathbf{k}_0)\cdot\mathbf{r}_j} - \frac{1}{2}\Gamma f(r)[e^{-i\mathbf{k}\cdot\mathbf{r}_2}e^{i\mathbf{k}_0\cdot\mathbf{r}_1} \pm (1\leftrightarrow 2)]\right], \tag{26}$$

with $a_\pm=\frac{1}{4}(\Gamma^{(2)}+\Gamma^{(1)})\pm x_{12}(r)$ and $x_{12}(r)=\sqrt{[(\Gamma^{(2)}-\Gamma^{(1)})/4]^2+\frac{1}{4}\Gamma^{(1)}\Gamma^{(2)}|f(r)|^2}$.

In the absence of collective effects $f(r)\to 0$, the initial phased-symmetric entangled state $|+\rangle_{\mathbf{k}_0}$ gives "quasidirectionality,"

$$C_{\mathbf{k}}(\infty)_{|+\rangle_{\mathbf{k}_0}} \simeq i\frac{1}{\sqrt{2}}\frac{g^*_{\mathbf{k}}}{\left(\frac{1}{2}\Gamma - i\Delta_{\mathbf{k}}\right)}\sum_{j=1,2} e^{-i(\mathbf{k}-\mathbf{k}_0)\cdot\mathbf{r}_j}. \tag{27}$$

The directionality becomes more obvious as j extends to a large integer, i.e., the summation approximates to a δ function.

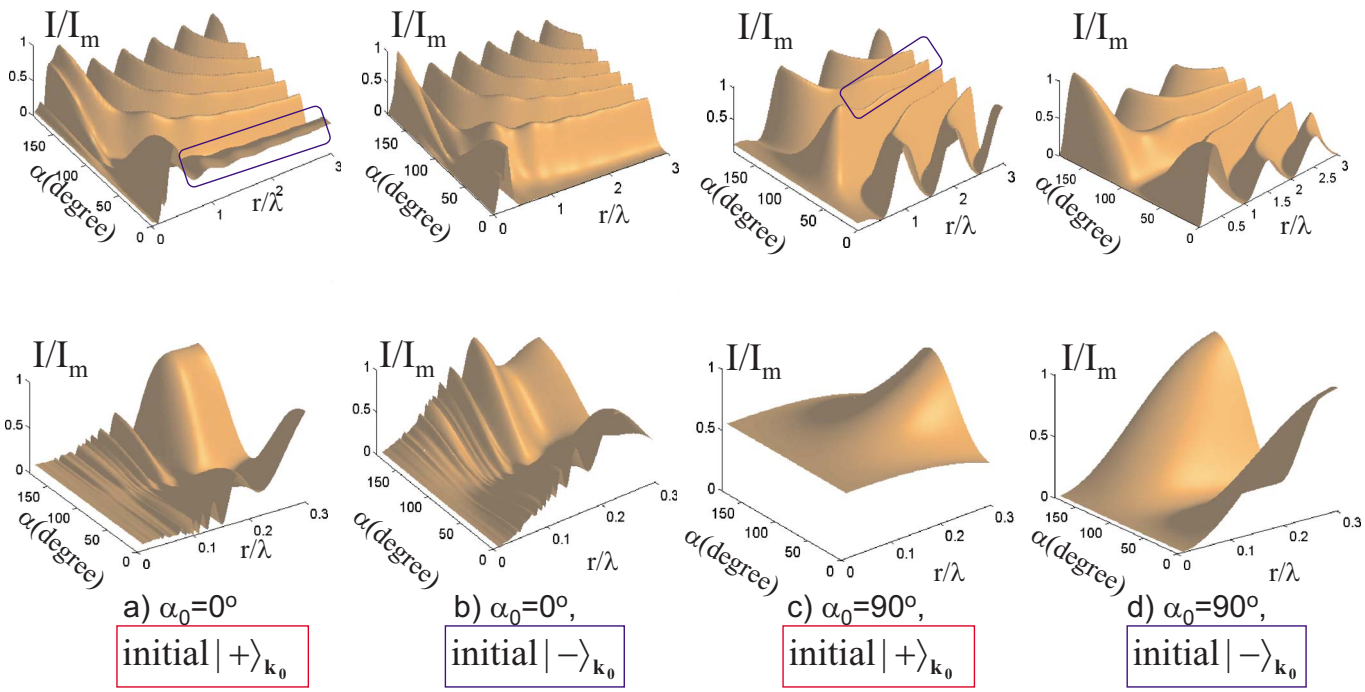

FIG. 6. (Color online) Directional dependence of the (normalized) intensity $I(r,\alpha)/I_m$ as a function of interatomic distance r and observation angle α for different angles of $\mathbf{k}_0$ for states $|\pm\rangle_{\mathbf{k}_0}=(1/\sqrt{2})(e^{i\mathbf{k}_0\cdot\mathbf{r}_1}|a_1,b_2\rangle\pm e^{i\mathbf{k}_0\cdot\mathbf{r}_2}|b_1,a_2\rangle)|0\rangle$. (a) $\alpha_0=0$ with initial phased-symmetric entangled state $|+\rangle_{\mathbf{k}_0}$, (b) $\alpha_0=0$ with initial phased-antisymmetric entangled state $|-\rangle_{\mathbf{k}_0}$, (c) $\alpha_0=90°$ with $|+\rangle_{\mathbf{k}_0}$, and (d) $\alpha_0=90°$ with $|-\rangle_{\mathbf{k}_0}$. The blue frame serves to highlight the directional correlation. The maximum value for all α and r is I_m. We have used $\Delta M=0$ transition.

III. PHOTON INTERFERENCE AND DIRECTIONAL EMISSION IN V SCHEME

The directional dependence of the photon emission for the V scheme (Sec. II C) can be analyzed appropriately by using the steady-state intensity $I(r_D,t_D)=\langle\Psi(\infty)|\hat{E}^\dagger(\mathbf{r}_D,t_D)\hat{E}(\mathbf{r}_D,t_D)|\Psi(\infty)\rangle=|\Psi^{(1)}(\mathbf{r}_D,t_D)|^2$. The amplitude of the photon field observed at space-time point $(\mathbf{r}_D,t_D)$ of a detector D is obtained after straightforward calculations along the lines of Ref. [18] as

$$\Psi^{(1)}(\mathbf{r}_D,t_D)_{|y\rangle_{\mathbf{k}_0}}=-\frac{1}{\sqrt{2}}\frac{\wp k^2}{4\pi\varepsilon_0}\left((K_-e^{\Gamma f\tau_1/2}+K_+e^{-\Gamma f\tau_1/2})\frac{1}{r_1}e^{-(i\omega+\Gamma/2)\tau_1}\Theta(\tau_1)+(K_+e^{-\Gamma f\tau_2/2}-K_-e^{\Gamma f\tau_2/2})\frac{1}{r_2}e^{-(i\omega+\Gamma/2)\tau_2}\Theta(\tau_2)\right) \quad (28)$$

with

$$K_\pm=e^{i\mathbf{k}_0\cdot\mathbf{r}_1}\pm ye^{i\mathbf{k}_0\cdot\mathbf{r}_2}=e^{i(k_0r/2)\cos\alpha_0}\pm ye^{-i(k_0r/2)\cos\alpha_0}, \quad (29)$$

where $y=\pm$ for the initial states $|\pm\rangle_{\mathbf{k}_0}$, α_0 is the angle between $\mathbf{k}_0$ and the interatomic axis [see Fig. 1(b)], $\tau_j=t_D-r_{Dj}/c$, and $r_{Dj}=|\mathbf{r}_D-\mathbf{r}_j|$ is the distance between the jth atom and detector D.

We show that the single-photon emission from an entangled state of two atoms gives the Young's interference for sufficiently large r such that $f(r)\to 0$. Here, Eq. (28) gives the intensity

$$I_{|\pm\rangle_{\mathbf{k}_0}}\propto\frac{e^{-\Gamma\tau_1}}{r_1^2}+\frac{e^{-\Gamma\tau_2}}{r_2^2}\pm\frac{e^{-\Gamma(\tau_1+\tau_2)/2}}{r_1r_2}2\cos(kr_{12}+\Phi_0), \quad (30)$$

where $\Phi_0(r)=k_0r\cos\alpha_0$ is the phase due to the initial exciting laser, $r_{21}=r_{D1}-r_{D2}$, and $k=\omega/c$. Assuming that $r_1=r_2$ and taking $\Phi_0=0$, for the symmetric state $(y=+)$, we have $K_+=2$, $K_-=0$ and hence $I_{|+\rangle}\propto\cos^2(\frac{1}{2}kr_{21})$. Thus, the interference pattern for the initial symmetric entangled state for $kr\gg 1$ is basically identical to the usual classical *Young's interference*. For an antisymmetric entangled state $(y=-)$, we have $K_-=2$, $K_+=0$, and hence $I_{|-\rangle}\propto\sin^2(\frac{1}{2}kr_{21})$ gives the *non-*

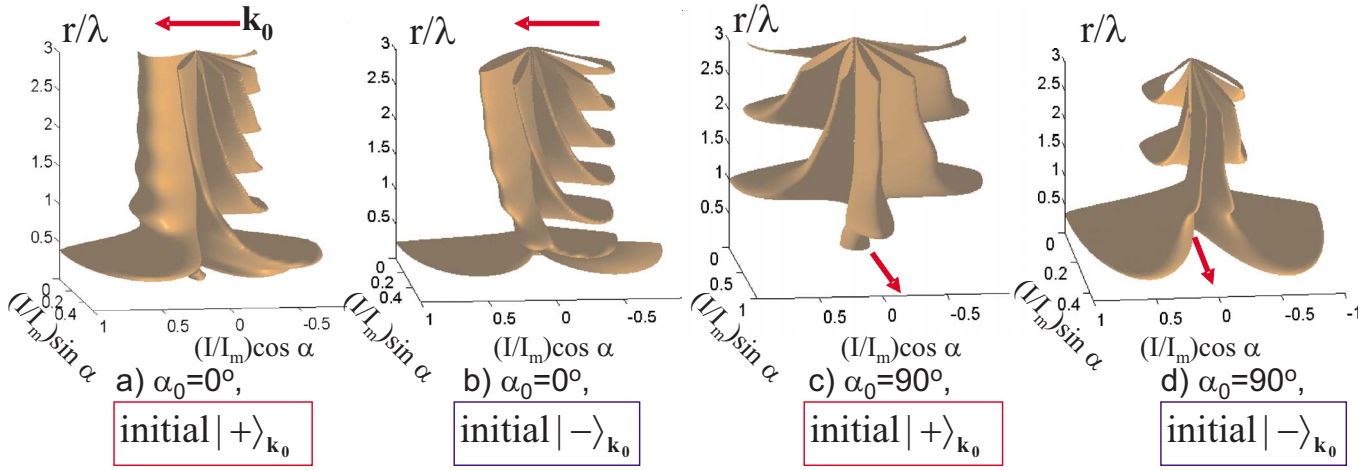

FIG. 7. (Color online) Same as Fig. 6 but in cylindrical coordinate system. The red arrows indicate the direction of the excitation laser, $\mathbf{k}_0$.

classical interference with a zero at $r_{21}=0$. This is much like the *Hong-Ou-Mandel* effect [19] or antibunching where there is a destructive interference when the path difference is zero.

When Φ_0 is finite, the interference pattern is simply shifted depending on Φ_0 and the phased-antisymmetric entangled state $|-\rangle_{\mathbf{k}_0}$ given by Eq. (24) may not give nonclassical interference. The amplitudes of the oscillations are the same in all directions since there is no diffraction effect from the two atoms. The relative initial phase $\Phi_0(r)$ between the two atoms gives the same effect as the scattering by an incoming plane wave.

The directional dependence of the intensity $I(\alpha,r)$ is plotted in Fig. 6 as a function of interatomic distance $r=|\mathbf{r}_1-\mathbf{r}_2|$ and detection angle α [defined in Fig. 1(b)] using Eq. (28). For large r, the directionality for symmetric entangled state [Figs. 6(a), 6(c), 7(a), and 7(c)] is manifested by a peak (spine or ridge) along the direction of incident $\mathbf{k}_0$, which spans almost the entire value of r, down to 0.5λ. Similar features are found for the antisymmetric state [Figs. 6(b), 6(d), 7(b), and 7(d)], except that there is a valley instead of a peak which spans almost the entire value of r. Here, the interference pattern is *sinelike* as opposed to the classical interference. This is the result of *destructive* interference due to the opposite phases of the two atoms. Thus, the *directional correlation* and *anticorrelation* are due to constructive and destructive quantum interference, respectively. The polar plots in Fig. 7 provide a much more intuitive picture of the directional dependence.

The directional correlation ceases when the atoms come too close (bottom panel of Fig. 6), i.e., $r \lesssim \lambda/2$. In this regime, the two atoms are not independent but they are coupled via *dipole-dipole interaction*. The emission intensity is much reduced since the radiation which normally gives rise to irreversible dissipation now creates reversible coherent interaction via the dipole-dipole interaction. When $\alpha_0=90°$ the emission is isotropic for both asymmetric and symmetric states, as if from a single atom. But the radiation goes to zero for the asymmetric state when $r\to 0$. When $\alpha_0=0$, the two atoms acquire a finite relative phase that depends on r. The phase is transferred between the two atoms as driven by the coherent dipole-dipole coupling, which causes a rapid variation of the intensity across r with no radiation orthogonal to the interatomic axis. The directions of the emitted photon are not correlated to $\mathbf{k}_0$. Further details of the directional property of emitted photons from three and more entangled atoms will be reported elsewhere [20].

IV. TWO-PHOTON CORRELATION

We proceed to calculate the two-photon correlation $G^{(2)}=|\psi(B,A)+\psi(A,B)|^2$, where the two-photon amplitude $\psi(B,A)$ is related to $C_{\mathbf{kq}}(\infty)$ by [18]

$$\psi(B,A)=\sum_{\mathbf{kq}} C_{\mathbf{k},\mathbf{q}}(\infty)\frac{\hbar\sqrt{\nu_{\mathbf{k}}\nu_{\mathbf{q}}}}{2\varepsilon_0 V}(\hat{\epsilon}_2\cdot\hat{\varepsilon}_{\mathbf{q}}) \times(\hat{\epsilon}_1\cdot\hat{\varepsilon}_{\mathbf{k}})e^{i(\mathbf{k}\cdot\mathbf{r}_A-\nu_{\mathbf{k}}t_A)}e^{i(\mathbf{q}\cdot\mathbf{r}_B-\nu_{\mathbf{q}}t_B)}. \quad (31)$$

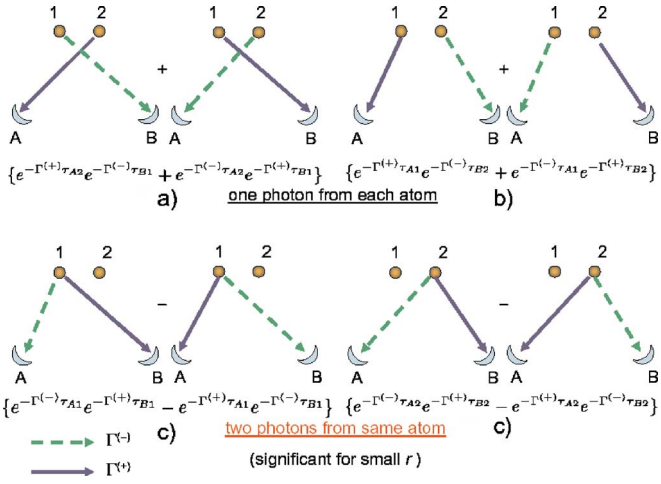

FIG. 8. (Color online) Schematic showing the four possible paths of photons from the two atoms to the detectors, corresponding to all the terms in the two-photon amplitude Eq. (32). The paths (c) and (d) arise when the interatomic distance r is small compared to the transition wavelength.

By assuming $\Sigma_\lambda(\epsilon^*_{\mathbf{k}\lambda}\epsilon_{\mathbf{k}\lambda})(\epsilon^*_{\mathbf{q}\lambda}\epsilon_{\mathbf{q}\lambda})\simeq 1$ and using $\Sigma_{\mathbf{k}}\to\Sigma_\lambda[V/(2\pi c)^3]\int_0^\infty \nu_{\mathbf{k}}^2 d\nu_{\mathbf{k}}\int_0^\pi d\theta\sin\theta\int_0^{2\pi}d\varphi$, we evaluate the integrations over $\mathbf{k}$ and $\mathbf{q}$. After lengthy algebra along the lines of Ref. [18], we obtain the far-field expression for the two-photon amplitude

$$\begin{aligned}\psi(B,A) = K_0\Bigg(&-\frac{1}{r_{A2}}\frac{1}{r_{B1}}e^{-i\omega(\tau_{A2}+\tau_{B1})}\Theta(\tau_{A2})\Theta(\tau_{B1})(e^{-\tilde{\Gamma}^{(+)}\tau_{A2}/2}e^{-\tilde{\Gamma}^{(-)}\tau_{B1}/2}+e^{-\tilde{\Gamma}^{(-)}\tau_{A2}/2}e^{-\tilde{\Gamma}^{(+)}\tau_{B1}/2})\\&-\frac{1}{r_{A1}}\frac{1}{r_{B2}}e^{-i\omega(\tau_{A1}+\tau_{B2})}\Theta(\tau_{A1})\Theta(\tau_{B2})(e^{-\tilde{\Gamma}^{(+)}\tau_{A1}/2}e^{-\tilde{\Gamma}^{(-)}\tau_{B2}/2}+e^{-\tilde{\Gamma}^{(-)}\tau_{A1}/2}e^{-\tilde{\Gamma}^{(+)}\tau_{B2}/2})\\&-\frac{1}{r_{A1}}\frac{1}{r_{B1}}e^{-i\omega(\tau_{A1}+\tau_{B1})}\Theta(\tau_{A1})\Theta(\tau_{B1})(e^{-\tilde{\Gamma}^{(-)}\tau_{A1}/2}e^{-\tilde{\Gamma}^{(+)}\tau_{B1}/2}-e^{-\tilde{\Gamma}^{(+)}\tau_{A1}/2}e^{-\tilde{\Gamma}^{(-)}\tau_{B1}/2})\\&-\frac{1}{r_{A2}}\frac{1}{r_{B2}}e^{-i\omega(\tau_{A2}+\tau_{B2})}\Theta(\tau_{A2})\Theta(\tau_{B2})(e^{-\tilde{\Gamma}^{(-)}\tau_{A2}/2}e^{-\tilde{\Gamma}^{(+)}\tau_{B2}/2}-e^{-\tilde{\Gamma}^{(+)}\tau_{A2}/2}e^{-\tilde{\Gamma}^{(-)}\tau_{B2}/2})\Bigg)\end{aligned} \tag{32}$$

with the emission times

$$\tau_{Aj}=t_A-\frac{r_{Aj}}{c},\quad \tau_{Bj}=t_B-\frac{r_{Bj}}{c}, \tag{33}$$

and distances from detector D to atom 1 or 2

$$r_{D1}=\sqrt{\left(r_{Dz}-\frac{1}{2}r\right)^2+r_{Dx}^2},\quad r_{D2}=\sqrt{\left(r_{Dz}+\frac{1}{2}r\right)^2+r_{Dx}^2}, \tag{34}$$

where $r_{Dx}=r_D\sin\alpha_D$, $r_{Dz}=r_D\cos\alpha_D$, $\Theta(x)$ is the Heaviside step function, and $K_0=2\wp^*\wp^*\omega^4/(4\pi\varepsilon_0c^2)^2$. The physics behind each term in Eq. (32) is shown by the diagrams in Fig. 8. The last two lines of Eq. (32), which correspond to Figs. 8(c) and 8(d), are important only at small r. These terms seem rather counterintuitive: that two photons are emitted from the same atom. In fact, it is the dipole-dipole interaction which excites the same atom and cause it to emit the second photon. Also, note that there is no step function of the form $\Theta(\tau_{A2}-\tau_{B1})$ because the two photons are not emitted sequentially although the form of Eq. (15) is identical to the cascade scheme.

For $\alpha_D=90°$ we have $r_{Dj}=r_0$; the amplitude becomes $\psi(1,2)=-(4K_0/r_0^2)\Theta(\tau_{A2})\Theta(\tau_{B1})e^{-i\omega(2\tau_A+\tau)}e^{-\Gamma\tau_A}e^{-\tilde{\Gamma}^{(+)}\tau/2}$, and we have the correlation, which decays exponentially,

$$G^{(2)}(\tau)=\left(\frac{4K_0}{r_0^2}\right)^2e^{-2\Gamma\tau_A}e^{-\Gamma(1+g(r))\tau}, \tag{35}$$

where $\tau_B=\tau_A+\tau$. The plot of Eq. (35) is shown in Fig. 9(b).

A. Large atomic separation

In the limit of large r we have $g(r)$, $h(r)$, $f(r)\to 0$ and $\tilde{\Gamma}^{(+)}\simeq\tilde{\Gamma}^{(-)}$, so the last two terms of Eq. (32), which correspond to the paths from each atom to the two detectors, are zero, i.e., the paths on the right of Figs. 8(c) and 8(d) are identical to (and cancel) those on the left. Only the first two terms of Eq. (32) are finite, leaving

$$\psi(B,A)=-2K_0\left(\frac{\Theta(\tau_{A2})\Theta(\tau_{B1})}{r_{A2}r_{B1}}e^{-(i\omega+\Gamma/2)(\tau_{A2}+\tau_{B1})}+\frac{\Theta(\tau_{A1})\Theta(\tau_{B2})}{r_{A1}r_{B2}}e^{-(i\omega+\Gamma/2)(\tau_{A1}+\tau_{B2})}\right). \tag{36}$$

For $\alpha_A=0°$, $\alpha_B=180°$ as in Fig. 9(a), we have $r_{Ax}=r_{Bx}=0$, $r_{Az}=r_A$, $r_{Bz}=-r_B$. When $r_D\sim r$ the correlation becomes

$$G^{(2)}(r,\tau)=G_0e^{-\Gamma\tau}\left|\frac{e^{(i\omega+\Gamma/2)r/c}}{r_A^+r_B^+}+\frac{e^{-(i\omega+\Gamma/2)(r/c)}}{r_A^-r_B^-}\right|^2 \tag{37}$$

where $G_0=(2K_0)^2e^{-2\Gamma(t_A-(r_A+r_B)/2c)}$ and $r_D^\pm=r_D\pm\frac{1}{2}r$. For $r_D\gg r$ we have

$$G^{(2)}(r,\tau)=\frac{G_0e^{-\Gamma\tau}}{(r_Ar_B)^2}2[\cosh(\Gamma r/c)+\cos(2\omega r/c)]. \tag{38}$$

Typically $\Gamma\sim 10^8\ \mathrm{s}^{-1}$, $r\sim 10^{-7}$ m, so $\Gamma r/c\ll 1$ and the oscillation period is $r=\lambda/2$. Thus, when the atoms and the detectors are in one line, Fig. 9(a) shows that interference of the two photons leads to a zero correlation when r is an odd multiples of $\lambda/4$.

For $\alpha_D=90°$ Eq. (35) reduces to

$$G^{(2)}(\tau)=\left(\frac{4K_0}{r_0^2}\right)^2e^{-2\Gamma\tau_A}e^{-\Gamma(1+g(r))\tau}. \tag{39}$$

B. Small atomic separation: Subwavelength resolutions

The two-photon correlation displays interesting features when the atoms and detectors are in one line [Fig. 9(a)], i.e., photon bunching with oscillations which become more rapid as r decreases.

When r is sufficiently small ($r \lesssim \lambda/8$ or $kr \lesssim \pi/4$) such that $g(r) \simeq 1$, all paths in Fig. 8 contribute and after replacing $\tilde{\Gamma}^{(+)} = (2\Gamma + i\Gamma h)$, $\tilde{\Gamma}^{(-)} = -i\Gamma h$ we have

$$\begin{aligned}\psi(1,2) \simeq K_0 \Bigg(& -\frac{\Theta(\tau_{A2})\Theta(\tau_{B1})}{r_{A2} r_{B1}} e^{-i\omega(\tau_{A2}+\tau_{B1})} (e^{-\Gamma\tau_{A2}} e^{-i\Gamma h(\tau_{A2}-\tau_{B1})/2} + e^{-\Gamma\tau_{B1}} e^{i\Gamma h(\tau_{A2}-\tau_{B1})/2}) \\ & - \frac{\Theta(\tau_{A1})\Theta(\tau_{B2})}{r_{A1} r_{B2}} e^{-i\omega(\tau_{A1}+\tau_{B2})} (e^{-\Gamma\tau_{A1}} e^{-i\Gamma h(\tau_{A1}-\tau_{B2})/2} + e^{-\Gamma\tau_{B2}} e^{i\Gamma h(\tau_{A1}-\tau_{B2})/2}) \\ & - \frac{\Theta(\tau_{A1})\Theta(\tau_{B1})}{r_{A1} r_{B1}} e^{-i\omega(\tau_{A1}+\tau_{B1})} (e^{-\Gamma\tau_{B1}} e^{i\Gamma h(\tau_{A1}-\tau_{B1})/2} - e^{-\Gamma\tau_{A1}} e^{-i\Gamma h(\tau_{A1}-\tau_{B1})/2}) \\ & - \frac{\Theta(\tau_{A2})\Theta(\tau_{B2})}{r_{A2} r_{B2}} e^{-i\omega(\tau_{A2}+\tau_{B2})} (e^{-\Gamma\tau_{B2}} e^{i\Gamma h(\tau_{A2}-\tau_{B2})/2} - e^{-\Gamma\tau_{A2}} e^{-i\Gamma h(\tau_{A2}-\tau_{B2})/2}) \Bigg). \end{aligned} \tag{40}$$

If we arranged the detectors such that $\tau_{A1} = \tau_{B1} = \tau_a$ and $\tau_{A2} = \tau_{B2} = \tau_b = \tau_a + \tau$, there would be no correlation $G^{(2)} = 0$. However, if we arrange the detectors with $\tau_{A2} = \tau_{B1} = \tau_a$ and $\tau_{A1} = \tau_{B2} = \tau_b = \tau_a + \tau$, we have $\psi(1,2) = (-2K_0/r_A r_B) \times (e^{-i2\omega\tau_a} e^{-\Gamma\tau_a} + e^{-i2\omega\tau_b} e^{-\Gamma\tau_b})$ and hence

$$G^{(2)}(r,\tau) = \left(\frac{2K_0}{r_A r_B}\right)^2 e^{-2\Gamma\tau_a} [1 + e^{-2\Gamma\tau} + 2e^{-\Gamma\tau} \cos(2\omega\tau)], \tag{41}$$

where we have assumed $r_{Dj} \simeq r_D$ in the denominators. When $\Gamma\tau_{a,b} \ll 1$, the oscillations become so rapid that the period is extremely small, $\tau\Gamma = \lambda\Gamma/2c \sim 10^{-7}$.

Equation (40) contains oscillatory terms governed by Γh, the dipole-dipole interaction strength. The physical origin is the periodic emission and reabsorption of a photon between the two atoms, giving rise to an induced coherent field that creates oscillations between the collective states $|a_1, b_2, 1_{\mathbf{k}}\rangle$ and $|a_1, b_2, 1_{\mathbf{k}}\rangle$. For $kr \ll 1$, the period of oscillations varies as $(kr)^3/\Gamma$ and the number of oscillations in one lifetime Γ^{-1} is $1/(kr)^3$ [21].

This oscillatory feature can be useful for resolving two atoms or molecules separated by a subwavelength distance. Our present approach for resolution is in time domain and useful information can be readily extracted from the measured temporal correlation. This is different from that of Refs. [22,23] which uses the spectral information of resonance fluorescence and the two-photon correlation. Further analysis will be presented elsewhere.

C. Angular correlation

The angular correlation between two successively emitted photons is plotted in Fig. 10 using Eq. (32). The ridges around $\alpha_B = 0°$ and $\alpha_B = 90°$ in Figs. 10(a) and 10(b) clearly show the angular correlation of the two photons for $\alpha_A = 0°$ and $\alpha_A = 90°$. For other angles of α_B, the correlation oscillates between zero and a maximum. For $r \ll \lambda/2$, the correlation is isotropic and essentially independent of the locations of the detectors. When both detectors are at right angles in Fig. 10(b), the correlation peaks at $r = \lambda, 2\lambda, \ldots$. When both detectors and the atoms are in one line, the correlation peaks at $r = \lambda/2, \lambda, 3\lambda/2, \ldots$. The oscillations become more rapid due to the interference of signals from the two detectors.

V. CONCLUSION

We have studied the collective dynamics of a two-atom system. We find that the dipole-dipole interaction induces a finite quantum coherence between the two intermediate states $|a_1, b_2, 1_{\mathbf{k}}\rangle$ and $|b_1, a_2, 1_{\mathbf{k}}\rangle$. At large times, a residual population due to coherence trapping is found in the state $|-\rangle$ for $r \sim \lambda/4$. The scalar photon model provides an intuitive picture to explain the equal populations in $|-\rangle$ and $|+\rangle$ for $r = n\lambda/2$. The effect of the second photon emission on the populations versus r can be seen by comparing the full $\diamond$ scheme and the Λ scheme. Single-photon interference is present in the V scheme but absent in the Λ scheme.

We have shown the directional emission of a single photon from two atoms prepared in the phased-symmetric and phased-antisymmetric entangled states by a laser pulse. The antisymmetric entangled state $|-\rangle_{\mathbf{k}_0}$ gives anticorrelation in the directionality. The photon emission becomes less directional and more isotropic at subwavelength atomic separation. The results are furnished with three-dimensional plots that provide a more intuitive picture than textual descriptions. In the absence of the position-dependent phase (due to excitation by a laser pulse) and large separation, the photon distribution gives Young's interference.

An analytical expression for the two-photon correlation $G^{(2)}$ has been derived. We found that it is possible for each atom to emit *two* photons due to the dipole-dipole interaction. We have analyzed the temporal correlation $G^{(2)}(\tau)$ as well as the directional correlation $G^{(2)}(\alpha_A, \alpha_B)$ between two photons from the two atoms prepared in the state $|a_1, a_2, 0\rangle$. For detectors arranged along the interatomic axis, the $G^{(2)}(\tau)$ profile shows oscillations with a period that depends on the atomic separation at subwavelength values. This feature could be useful for subwavelength metrology. Antibunching is found when $r = \lambda/4$, where one atom is on a node and another on the antinode of the photon field with the two possibilities giving rise to destructive interference. The an-

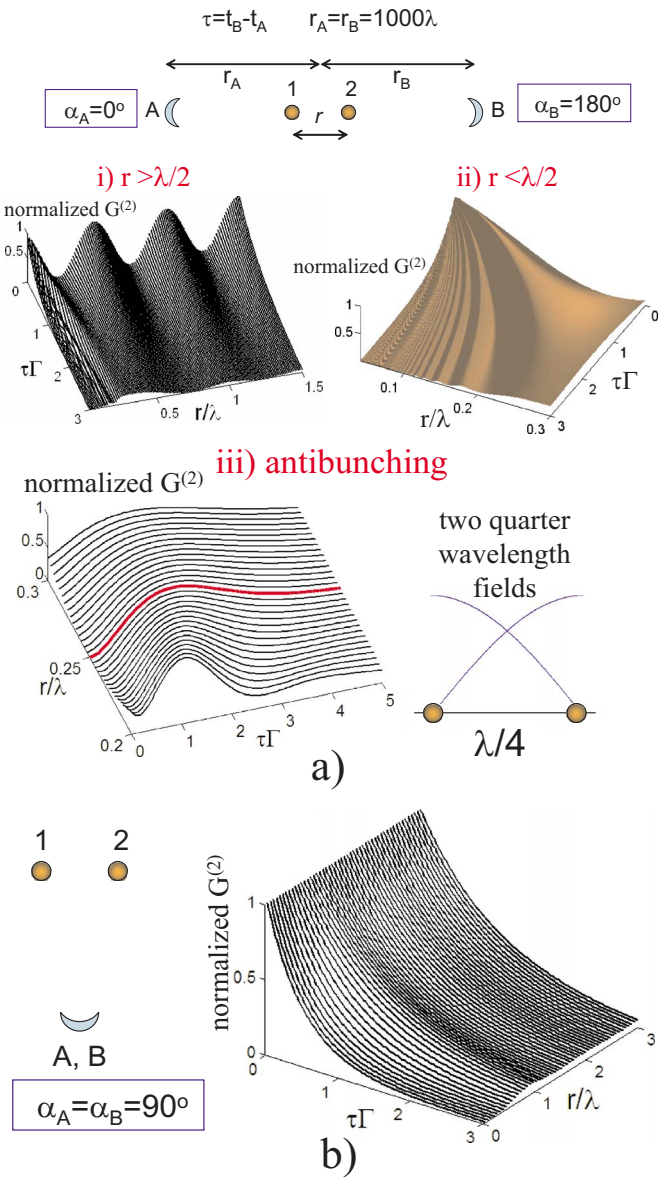

FIG. 9. (Color online) Two-photon temporal correlation $G^{(2)}(\tau)$ for different arrangements of detectors. (a) Detectors are along the interatomic axis ($\alpha_A=0°$, $\alpha_B=180°$). (i) Destructive interference of the photons from two atoms spaced by odd integral of $\lambda/2$ leads to zero correlation. (ii) For $r<\lambda/2$, oscillations appear and become more rapid as r decreases. The period of the oscillations decreases with increasing r, a useful feature for measuring subwavelength interatomic separation. (iii) Antibunching occurs around $r\simeq\lambda/4$ (highlighted by the red thick line) and can be understood as the destructive interference of two quarter waves. (b) Detectors are orthogonal to interatomic axis ($\alpha_A=\alpha_B=90°$). For large atomic separation, the correlation decays exponentially to zero with $\tau=t_B-t_A$. Another interesting feature around $r\sim\lambda/2$ is where the finite or nonzero correlation occurs at large τ. This is true even when the detectors are perpendicular to the interatomic axis. We have used the $\Delta M=0$ transition.

gular correlation between the two emitted photons found in $G^{(2)}(\alpha_A,\alpha_B)$ is similar to the directional correlation between the single emitted photon and the exciting photon $\mathbf{k}_0$ in the V scheme.

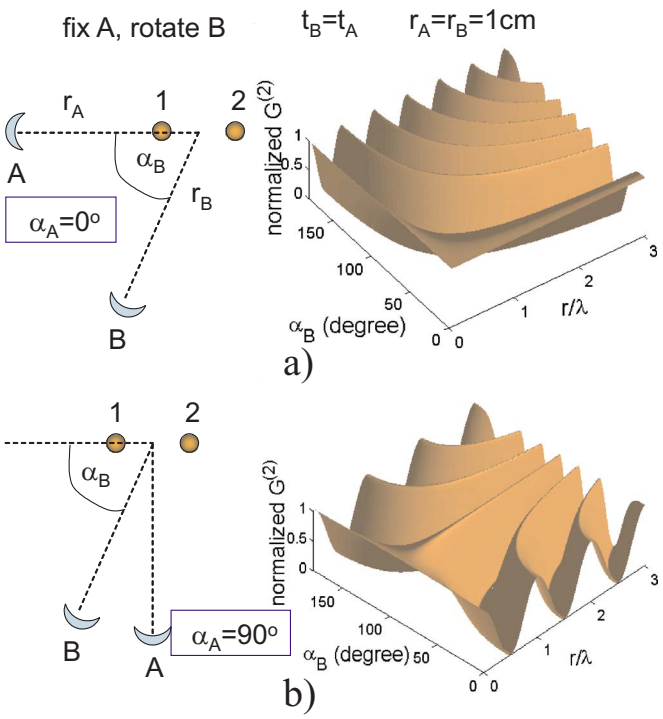

FIG. 10. (Color online) Angular correlation is clearly seen for both cases where the first detector is along the interatomic axis or perpendicular to it, as first predicted by Dicke. In addition, the features are richer. (a) At half integrals of a wavelength, the correlation vanishes in all directions due to destructive interference. (b) For $\lambda/2<r<\lambda$ there is clear angular correlation of the second photon to the first photon going to detector A. For $r\ll\lambda/2$, the correlation is isotropic. The correlation is zero at half-integral wavelength only when both detectors are at right angles due to destructive interference. We have used the $\Delta M=0$ transition.

Another interesting coherence effect of the collective system is that the dipole-dipole interaction can give rise to entanglement between two atoms. Detailed analysis of the entanglement between the two atoms using the density matrix equation and concurrence can be found in Ref. [24].

Finally, we briefly describe the possibility of experimental realization based on recent progress in the interest of nonclassical single-photon source. The generation of a single photon from a single atom [25] has been extended to two atoms. Photon antibunching has been observed from two independent sources that produce nondegenerate photon pairs [26], and from two independent atoms (in two optical traps) [4] as well as from two atomic ions localized down to 0.3 mm [27] that produce indistinguishable photons. These experiments may be adapted to test our results for large atomic separation. Certain aspects of Dicke's effect have been demonstrated [28] with two atoms at subwavelength separation embedded in a solid state matrix. Although the decoherence due to phonons does not impede the observation of the coherent effects, it is not favorable for the purpose of entanglement. Recently, two atoms with subwavelength separation have been successfully trapped in a single optical potential well [2]. This opens up the possibility for experimentally studying the collective or coherent effects of two atoms, particularly on the nature of emitted photons.

ACKNOWLEDGMENTS

R.O. would like to thank M. O. Scully, T. Becker, and I. Cirac for stimulating discussions while at MPQ and BK21 for support.

APPENDIX A: COUPLED EQUATIONS FOR FULL FOUR STATES SCHEME

The Hamiltonian Eq. (1) and the state vector Eq. (2) give the coupled equations

$$\frac{d}{dt}A(t) = i\sum_{\mathbf{k},j=1,2}\tilde{B}_{\mathbf{k}}^{(j)}(t)g_{\mathbf{k}}^{(j)}, \tag{A1}$$

$$\left(\frac{d}{dt}+i\Delta_{\mathbf{k}}\right)\tilde{B}_{\mathbf{k}}^{(1)}(t) = iA(t)g_{\mathbf{k}}^{(1)*}+i\sum_{\mathbf{q}}g_{\mathbf{q}}^{(2)}\tilde{C}_{\mathbf{kq}}(t), \tag{A2}$$

$$\left(\frac{d}{dt}+i\Delta_{\mathbf{k}}\right)\tilde{B}_{\mathbf{k}}^{(2)}(t) = iA(t)g_{\mathbf{k}}^{(2)*}+i\sum_{\mathbf{q}}g_{\mathbf{q}}^{(1)}\tilde{C}_{\mathbf{kq}}(t), \tag{A3}$$

$$\left(\frac{d}{dt}+i\Delta_{\mathbf{k}}+i\Delta_{\mathbf{q}}\right)\tilde{C}_{\mathbf{kq}}(t) = i[g_{\mathbf{k}}^{(1)*}\tilde{B}_{\mathbf{q}}^{(2)}(t)+g_{\mathbf{k}}^{(2)*}\tilde{B}_{\mathbf{q}}^{(1)}(t) + (\mathbf{k}\leftrightarrow\mathbf{q})], \tag{A4}$$

where $\tilde{B}_{\mathbf{k}}^{(j)}(t)=B_{\mathbf{k}}^{(j)}(t)e^{-i\Delta_{\mathbf{k}}t}$ and $\tilde{C}_{\mathbf{kq}}(t)=C_{\mathbf{kq}}(t)e^{-i\Delta_{\mathbf{k}}t}e^{-i\Delta_{\mathbf{q}}t}$. To simplify the notations, we have absorbed the important position-dependent factor $e^{i\mathbf{k}\cdot\mathbf{r}_j}$ into $g_{\mathbf{k}}^{(j)}$ and write them explicitly only if necessary, especially in the final results. The detailed calculations that give the results in the text will be presented elsewhere [29].

APPENDIX B: COLLECTIVE FACTORS g AND h

For linear polarization ($\Delta M=0$) where $\vec{\wp}\|\mathbf{r}_1-\mathbf{r}_2$,

$$g^{\|}(r) = \frac{3}{4}\int_0^{\pi}(\sin^3\theta)e^{\pm ik_0r\cos\theta}d\theta = 3\left(\frac{\sin a}{a^3}-\frac{\cos a}{a^2}\right) = \frac{3j_1(a)}{a} = j_0(a)+j_2(a), \tag{B1}$$

$$h^{\|}(r) = \frac{1}{2\pi\omega^3}\mathrm{P}\int_0^{\infty}g^{\|}(\nu r/c)\frac{\nu^3 d\nu}{\nu-\omega} = -3\left(\frac{\cos a}{a^3}+\frac{\sin a}{a^2}\right), \tag{B2}$$

where $a=k_0r$ and $k_0=\omega/c$.

For circular $\sigma^{\pm}$ polarization ($\Delta M=\pm1$) where $\vec{\wp}\perp(\mathbf{r}_1-\mathbf{r}_2)$,

$$g^{\perp}(r) = \frac{3}{4}\int_0^{\pi}\left(1-\frac{1}{2}\sin^2\theta\right)e^{\pm ik_0r\cos\theta}\sin\theta\,d\theta = \frac{3}{2}\left(\frac{\sin a}{a}+\frac{\cos a}{a^2}-\frac{\sin a}{a^3}\right) = j_0(a)-\frac{1}{2}j_2(a), \tag{B3}$$

$$h^{\perp}(r) = \frac{3}{2}\left(-\frac{\cos a}{a}+\frac{\sin a}{a^2}+\frac{\cos a}{a^3}\right). \tag{B4}$$

If we assume scalar photon (as discussed in Sec. II A 6), $\Sigma_{\lambda=1,2}\epsilon_{\mathbf{k}\lambda p}\epsilon_{\mathbf{k}\lambda p}^{*}=1$ gives a simpler expression,

$$g(r) = \frac{1}{2}\int_0^{\pi}(\sin\theta)e^{\pm ik_0r\cos\theta}d\theta = \frac{\sin(a)}{a} = \frac{1}{3}g^{\|}(a)+\frac{2}{3}g^{\perp}(a), \tag{B5}$$

which provides better insights into the physics.

The importance of the $h(r)$ function is elaborated as follows. It has been shown [30] that the energy shift becomes significantly larger when the interatomic distance is less than the wavelength, $r<\lambda$. The contribution of the principal parts to the interaction energy or level shift can only be evaluated correctly without the rotating wave approximation, and has been derived by Stephen [6] using a minimal coupling Hamiltonian, Lehmberg [31], and Milonni and Knight [10] using multipolar Hamiltonians, and Agarwal using both formalisms [32]. Arrechi and Courtens [8] have considered emission only in a single direction, where the angular integration in $\Sigma_{\mathbf{k}}$ is not taken into account. As pointed out by Milonni and Knight [10], this is unrealistic and would not give the correct result concerning the directionality.

APPENDIX C: TWO-ATOM Λ SCHEME

In this appendix, we give the theory for the Λ scheme shown in Fig. 4. The state vector can be written as

$$|\Psi(t)\rangle = A|a_1,a_2,0\rangle+\sum_{\mathbf{k}}[B_{\mathbf{k}}^{(2)}(t)|a_1,b_2\rangle+B_{\mathbf{k}}^{(1)}(t)|b_1,a_2\rangle]|1_{\mathbf{k}}\rangle. \tag{C1}$$

This corresponds to the collective four-level scheme where we disregard the ground state with two photons. We then have a three-state Λ system with the corresponding coupled equations

$$\frac{d}{dt}A(t) = i\sum_{\mathbf{k}}[\tilde{B}_{\mathbf{k}}^{(1)}(t)g_{\mathbf{k}}^{(2)}+\tilde{B}_{\mathbf{k}}^{(2)}(t)g_{\mathbf{k}}^{(1)}], \tag{C2}$$

$$\frac{d}{dt}\tilde{B}_{\mathbf{k}}^{(1)}(t) = -i\Delta_{\mathbf{k}}\tilde{B}_{\mathbf{k}}^{(1)}(t)+iA(t)g_{\mathbf{k}}^{(2)*}, \tag{C3}$$

$$\frac{d}{dt}\tilde{B}_{\mathbf{k}}^{(2)}(t) = -i\Delta_{\mathbf{k}}\tilde{B}_{\mathbf{k}}^{(2)}(t)+iA(t)g_{\mathbf{k}}^{(1)*}, \tag{C4}$$

where $\tilde{B}_{\mathbf{k}}^{(j)}(t)=B_{\mathbf{k}}^{(j)}(t)e^{-i\Delta_{\mathbf{k}}t}$.

The Laplace transform method gives the solutions

$$A(t) = A(0)e^{-Gt}, \tag{C5}$$

$$B_{\mathbf{k}}^{(1,2)}(t) = -A(0)g_{\mathbf{k}}^{(2,1)*}\frac{1-e^{i\Delta_{\mathbf{k}}t}e^{-Gt}}{\Delta_{\mathbf{k}}+iG}, \tag{C6}$$

where $G=\Sigma_{\mathbf{k}}(|g_{\mathbf{k}}^{(2)}|^2+|g_{\mathbf{k}}^{(1)}|^2)/s+i\Delta_{\mathbf{k}}=\frac{1}{2}(\Gamma^{(1)}+\Gamma^{(2)})$ with the spontaneous decay rates $\Gamma^{(j)}=2\pi|g_{\omega}^{(j)}|^2D(\omega)$

$=\omega^3|\wp^{(j)}|^2/3\pi\varepsilon_0\hbar c^3$. By defining the coefficients $B_{\pm\mathbf{k}}(t)=(1/\sqrt{2})[B_{\mathbf{k}}^{(1)}(t)\pm B_{\mathbf{k}}^{(2)}(t)]$ corresponding to the symmetric and antisymmetric states $|\pm\rangle=(1/\sqrt{2})(|a_1;b_2,1_{\mathbf{k}}\rangle\pm|b_1,1_{\mathbf{k}};a_2\rangle)$, we have

$$B_{\mathbf{k}}^{(\pm)}(t)=-\frac{A(0)}{\sqrt{2}}\frac{1-e^{i\Delta_{\mathbf{k}}t}e^{-Gt}}{\Delta_{\mathbf{k}}+iG}(g_{\mathbf{k}}^{(2)*}\pm g_{\mathbf{k}}^{(1)*}). \tag{C7}$$

We then have the probabilities given by Eq. (19). The single-photon amplitude $\Psi^{(1)}(\mathbf{r}_D,t_D)=\langle 0|\hat{E}(\mathbf{r}_D,t_D)|\Psi(\infty)\rangle$ in Eq. (20) can be calculated from

$$\Psi^{(1)}=\sum_{\mathbf{k},j=1,2}B_{\mathbf{k}}^{(j)}(\infty)\sqrt{\frac{\hbar\nu_{\mathbf{k}}}{2\varepsilon_0 V}}\hat{\epsilon}\cdot\hat{\varepsilon}_{\mathbf{k}}e^{i(\mathbf{k}\cdot\mathbf{r}_{Dj}-\nu_{\mathbf{k}}t_{Dj})} \tag{C8}$$

by using $A(0)=e^{i\mathbf{k}_0\cdot(\mathbf{r}_1+\mathbf{r}_2)}$, $g_{\mathbf{k}}^{(j)*}=\vec{\wp}^{(j)*}\cdot\hat{\varepsilon}_{\mathbf{k}}^*\sqrt{\nu_{\mathbf{k}}/2\varepsilon_0\hbar V}$ and

$$\frac{3}{4}\int_0^\pi N(\theta)\sin\theta e^{-i\mathbf{k}\cdot\mathbf{r}_{Dj}}d\theta=A_je^{ix}+A_j^*e^{-ix}=g(x), \tag{C9}$$

$$g^{\parallel}(x)=3\left(\frac{\sin x}{x^3}-\frac{\cos x}{x^2}\right), \tag{C10}$$

$$g^{\perp}(x)=\frac{3}{2}\left(\frac{\sin x}{x}+\frac{\cos x}{x^2}-\frac{\sin x}{x^3}\right), \tag{C11}$$

with $x=kr_{Dj}$ and $\parallel/\perp$ for linear (circular) ($\sigma^{\pm}$) polarizations, respectively.

APPENDIX D: TWO-ATOM V SCHEME

Here, we present the theory for the interaction of two atoms with free space radiation for the V scheme in Figs. 1(d) and 5. Here, the collective basis is the excited states without photon, $|a_1,b_2,0\rangle$ and $|b_1,a_2,0\rangle$ and the ground state $|b_1,b_2,1_{\mathbf{k}}\rangle$ with photon $\mathbf{k}$, and state $|a_1,a_2\rangle$ is not involved. The resulting state vector can be written as

$$|\Psi(t)\rangle=[B^{(2)}(t)|a_1,b_2\rangle+B^{(1)}(t)|b_1,a_2\rangle]|0\rangle+\sum_{\mathbf{k}}C_{\mathbf{k}}(t)|b_1,b_2,1_{\mathbf{k}}\rangle. \tag{D1}$$

The same basis in the state vector was considered by Arrechi and Courtens [8] in the context of propagation.

The set of equations then are

$$\frac{d}{dt}B^{(1)}(t)=i\sum_{\mathbf{k}}g_{\mathbf{k}}^{(2)}e^{i\mathbf{k}\cdot\mathbf{r}_2}e^{-i\Delta_{\mathbf{k}}t}C_{\mathbf{k}}(t), \tag{D2}$$

$$\frac{d}{dt}B^{(2)}(t)=i\sum_{\mathbf{k}}g_{\mathbf{k}}^{(1)}e^{i\mathbf{k}\cdot\mathbf{r}_1}e^{-i\Delta_{\mathbf{k}}t}C_{\mathbf{k}}(t), \tag{D3}$$

$$\frac{d}{dt}C_{\mathbf{k}}(t)=ig_{\mathbf{k}}^{(1)*}e^{-i\mathbf{k}\cdot\mathbf{r}_1}e^{i\Delta_{\mathbf{k}}t}B^{(2)}(t)+(1\leftrightarrow 2). \tag{D4}$$

Integrating Eq. (4) and replacing it into Eqs. (2) and (3) we have

$$\frac{d}{dt}B^{(1)}(t)\simeq i\sum_{\mathbf{k}}g_{\mathbf{k}}^{(2)}e^{i\mathbf{k}\cdot\mathbf{r}_2}e^{-i\Delta_{\mathbf{k}}t}C_{\mathbf{k}}(0)-\frac{1}{2}\sqrt{\Gamma^{(1)}\Gamma^{(2)}}f(r)B^{(2)}(t)-\frac{1}{2}\Gamma^{(2)}B^{(1)}(t), \tag{D5}$$

$$\frac{d}{dt}B^{(2)}(t)\simeq i\sum_{\mathbf{k}}g_{\mathbf{k}}^{(1)}e^{i\mathbf{k}\cdot\mathbf{r}_1}e^{-i\Delta_{\mathbf{k}}t}C_{\mathbf{k}}(0)-\frac{1}{2}\sqrt{\Gamma^{(1)}\Gamma^{(2)}}f(r)B^{(1)}(t)-\frac{1}{2}\Gamma^{(1)}B^{(2)}(t). \tag{D6}$$

The Laplace transform method is used to obtain the solutions

$$B^{(1)}(t)=\frac{\left(a_+-\frac{1}{2}\Gamma^{(1)}\right)e^{-a_+t}-\left(a_--\frac{1}{2}\Gamma^{(1)}\right)e^{-a_-t}}{x_{12}}B^{(1)}(0)+\frac{e^{-a_+t}-e^{-a_-t}}{x_{12}}\frac{1}{2}\sqrt{\Gamma^{(1)}\Gamma^{(2)}}f(r)B^{(2)}(0), \tag{D7}$$

$$B^{(2)}(t)=\frac{\left(a_+-\frac{1}{2}\Gamma^{(2)}\right)e^{-a_+t}-\left(a_--\frac{1}{2}\Gamma^{(2)}\right)e^{-a_-t}}{x_{12}}B^{(2)}(0)+\frac{e^{-a_+t}-e^{-a_-t}}{x_{12}}\frac{1}{2}\sqrt{\Gamma^{(1)}\Gamma^{(2)}}f(r)B^{(1)}(0), \tag{D8}$$

where $a_{\pm}=\frac{1}{4}(\Gamma^{(2)}+\Gamma^{(1)})\pm\frac{1}{2}x_{12}$ and $x_{12}=\sqrt{[(\Gamma^{(2)}-\Gamma^{(1)})/2]^2+\Gamma^{(1)}\Gamma^{(2)}f(r)^2}$. For $\Gamma^{(1)}=\Gamma^{(2)}$ we have $a_{\pm}=\frac{1}{2}\tilde{\Gamma}^{(\pm)}=\frac{1}{2}\Gamma\{1\pm f(r)\}$ and

$$B^{(\pm)}(t)=e^{-1/2\tilde{\Gamma}^{(\pm)}t}B^{(\pm)}(0) \tag{D9}$$

where $B^{(\pm)}(t)=(1/\sqrt{2})[B^{(1)}(t)\pm B^{(2)}(t)]$.

Assuming that $C_{\mathbf{k}}(0)=0$ we have the transient solution for the ground-state coefficient

$$C_{\mathbf{k}}(t)=i[K_{\mathbf{k}}(t)g_{\mathbf{k}}^{(1)*}e^{-i\mathbf{k}\cdot\mathbf{r}_1}-L_{\mathbf{k}}(t)g_{\mathbf{k}}^{(2)*}e^{-i\mathbf{k}\cdot\mathbf{r}_2}]B^{(2)}(0)+i[K_{\mathbf{k}}(t)g_{\mathbf{k}}^{(2)*}e^{-i\mathbf{k}\cdot\mathbf{r}_2}-L_{\mathbf{k}}(t)g_{\mathbf{k}}^{(1)*}e^{-i\mathbf{k}\cdot\mathbf{r}_1}]B^{(1)}(0), \tag{D10}$$

$$K_{\mathbf{k}}(t)=-\frac{1}{2}[m_{\mathbf{k}}^{+}(t)+m_{\mathbf{k}}^{-}(t)]+p_{\mathbf{k}}\frac{\left(i\Delta_{\mathbf{k}}-\frac{1}{2}\Gamma\right)}{\Gamma f(r)}$$

$$\text{and}\quad L_{\mathbf{k}}(t)=\frac{1}{2}[m_{\mathbf{k}}^{+}(t)-m_{\mathbf{k}}^{-}(t)-p_{\mathbf{k}}], \tag{D11}$$

where $m_{\mathbf{k}}^{\pm}(t)=e^{i\Delta_{\mathbf{k}}t}e^{-a_{\pm}t}/(a_{\pm}-i\Delta_{\mathbf{k}})$, $p_{\mathbf{k}}=1/(a_+-i\Delta_{\mathbf{k}})-1/(a_--i\Delta_{\mathbf{k}})=-\Gamma f(r)/(a_+-i\Delta_{\mathbf{k}})(a_--i\Delta_{\mathbf{k}})$.

The steady-state solution is

$$C_{\mathbf{k}}(\infty) = ip_{\mathbf{k}}g_{\mathbf{k}}^{*}\left[\left(\frac{i\Delta_{\mathbf{k}} - \frac{1}{2}\Gamma}{\Gamma f(r)}e^{-i\mathbf{k}\cdot\mathbf{r}_1} + \frac{1}{2}e^{-i\mathbf{k}\cdot\mathbf{r}_2}\right)B^{(2)}(0) + (1 \leftrightarrow 2)\right]. \quad \text{(D12)}$$

APPENDIX E: NO COHERENCE BETWEEN $|+\rangle$ and $|-\rangle$

The coherence can be calculated by first noting that $\rho_{-+} \doteq \langle -|\hat{\rho}(t)|+\rangle = \Sigma_{\mathbf{k},\mathbf{k}'} B_{\mathbf{k}}^{(-)}(t) B_{\mathbf{k}'}^{(+)*}(t) |1_{\mathbf{k}}\rangle\langle 1_{\mathbf{k}'}|$ where $\hat{\rho}(t) = |\Psi(t)\rangle\langle\Psi(t)|$. Then we calculate

$$\begin{aligned}\langle 1_{\mathbf{k}}, -|\hat{\rho}(t)|+, 1_{\mathbf{k}}\rangle &= B_{\mathbf{k}}^{(-)}(t)B_{\mathbf{k}}^{(+)*}(t) = \frac{1}{2}Z_{\mathbf{k}}(t)[|g_{\mathbf{k}}^{(1)}|^2 \\ &\quad + g_{\mathbf{k}}^{(1)*}g_{\mathbf{k}}^{(2)}e^{-i\mathbf{k}\cdot\mathbf{r}_{12}} - (1 \leftrightarrow 2)] \\ &\simeq \frac{1}{2}Z_{\mathbf{k}}(t)|g_{\mathbf{k}}|^2(e^{-i\mathbf{k}\cdot\mathbf{r}_{12}} - e^{i\mathbf{k}\cdot\mathbf{r}_{12}}) \quad \text{(E1)}\end{aligned}$$

where

$$Z_{\mathbf{k}}(t) = \frac{(e^{-\Gamma t} + e^{-i\Gamma ht}e^{-2\Gamma t} - e^{-i\Gamma ht/2}e^{-\Gamma t}2\cos\Delta_{\mathbf{k}}t)}{\left(i\Delta_{\mathbf{k}}^{+} - \frac{1}{2}\Gamma^{(+)}\right)\left(-i\Delta_{\mathbf{k}}^{-} - \frac{1}{2}\Gamma^{(-)}\right)}. \quad \text{(E2)}$$

The coherence is obtained by tracing (summing) over all wave vectors

$$\begin{aligned}\rho_{-+}(t) &= \frac{1}{2}\sum_{\mathbf{k}}|g_{\mathbf{k}}|^2(e^{-i\mathbf{k}\cdot\mathbf{r}_{12}} - e^{i\mathbf{k}\cdot\mathbf{r}_{12}})Z_{\mathbf{k}}(t) \\ &= \frac{-2i|\wp|^2c}{16\pi^2\varepsilon_0\hbar}\int_0^{\infty}Z_{\mathbf{k}}(t)k^3\int_0^{\pi}\sin(\mathbf{k}\cdot\mathbf{r}_{12})N(\theta)\sin\theta\, d\theta\, dk \\ &= \frac{|\wp|^2}{12\pi^2\varepsilon_0\hbar c^3}\int_{-\infty}^{\infty}Z_{\mathbf{k}}(t)v^3[g(vr/c) - g(vr/c)]dv = 0.\end{aligned} \quad \text{(E3)}$$

So there is no coherence between the symmetric and antisymmetric states.

[1] M. Gross and S. Haroche, Phys. Rep. **93**, 301 (1982).
[2] Y. Miroshnychenko, W. Alt, I. Dotsenko, L. Förster, M. Khudaverdyan, D. Meschede, S. Reick, and A. Rauschenbeutel, Phys. Rev. Lett. **97**, 243003 (2006).
[3] R. G. DeVoe and R. G. Brewer, Phys. Rev. Lett. **76**, 2049 (1996).
[4] J. Beugnon, M. P. A. Jones, J. Dingjan, B. Darquie, G. Messin, A. Browaeys, and P. Grangier, Nature (London) **440**, 779 (2006).
[5] R. H. Dicke, Phys. Rev. **93**, 99 (1954).
[6] M. J. Stephen, J. Chem. Phys. **40**, 669 (1964).
[7] V. Ernst and P. Stehle, Phys. Rev. **176**, 1456 (1968).
[8] F. T. Arecchi and E. Courtens, Phys. Rev. A **2**, 1730 (1970).
[9] R. H. Lehmberg, Phys. Rev. A **2**, 889 (1970).
[10] P. W. Milonni and P. L. Knight, Phys. Rev. A **10**, 1096 (1974).
[11] R. Bonifacio and G. Preparata, Phys. Rev. A **2**, 336 (1970).
[12] M. O. Scully, E. S. Fry, C. H. Raymond Ooi, and K. Wodkiewicz, Phys. Rev. Lett. **96**, 010501 (2006).
[13] C. H. Raymond Ooi, Phys. Rev. A **75**, 043818 (2007).
[14] L. I. Men'shikov, Phys. Usp. **42**, 107 (1999).
[15] M. O. Scully and M. S. Zubairy, *Quantum Optics* (Cambridge University Press, Cambridge, U.K., 1997).
[16] D. Kleppner, Phys. Rev. Lett. **47**, 233 (1981).
[17] Suppose that the system is in the state $|+\rangle_{\mathbf{k}_0}$ when the atoms are at points $(\mathbf{r}_1, \mathbf{r}_2)$. Then, when the atoms are at points $(\mathbf{r}_1, \mathbf{r}_2')$ with $\mathbf{k}_0\cdot(\mathbf{r}_2' - \mathbf{r}_2) = \pm\pi, \pm 3\pi, \ldots$, the system is in the state $|-\rangle_{\mathbf{k}_0}$.
[18] C. H. Raymond Ooi, A. K. Patnaik, and M. O. Scully, Proc. SPIE **5846**, 204 (2005).
[19] C. K. Hong, Z. Y. Ou, and L. Mandel, Phys. Rev. Lett. **59**, 2044 (1987).
[20] B.-G. Kim, C. H. Raymond Ooi, and H.-W. Lee (unpublished).
[21] The cubic dependence is due to the vectorial nature of the photon. One would have linear dependence if scalar photons were assumed.
[22] J.-T. Chang, Jörg Evers, M. O. Scully, and M. S. Zubairy, Phys. Rev. A **73**, 031803(R) (2006).
[23] J.-T. Chang, Jörg Evers, and M. S. Zubairy, Phys. Rev. A **74**, 043820 (2006).
[24] Z. Ficek and R. Tanaś, Phys. Rev. A **74**, 024304 (2006).
[25] M. Hijlkema *et al.*, Nat. Phys. **3**, 253 (2007);J. Volz, M. Weber, D. Schlenk, W. Rosenfeld, J. Vrana, K. Saucke, C. Kurtsiefer, and H. Weinfurter, Phys. Rev. Lett. **96**, 030404 (2006); Science **309**, 454 (2005); B. B. Blinov, D. L. Moehring, L.-M. Duan, and C. Monroe, Nature (London) **428**, 153 (2004).
[26] H. de Riedmatten, I. Marcikic, W. Tittel, H. Zbinden, and N. Gisin, Phys. Rev. A **67**, 022301 (2003).
[27] P. Maunz, D. L. Moehring, M. J. Madsen, R. N. Kohn, Jr., K. C. Younge, and C. Monroe, e-print arXiv:quant-ph/0608047.
[28] C. Hettich, C. Schmitt, J. Zitzmann, S. Kühn, I. Gerhardt, and V. Sandoghdar, Science **298**, 385 (2002).
[29] C. H. Raymond Ooi, Y. Rostovtsev, and M. O. Scully, Laser Phys. **17**, 1 (2007).
[30] C. Skornia, J. von Zanthier, G. S. Agarwal, E. Werner, and H. Walther, Phys. Rev. A **64**, 053803 (2001).
[31] R. H. Lehmberg, Phys. Rev. A **2**, 883 (1970).
[32] G. S. Agarwal, *Quantum Optics*, Springer Tracts in Modern Physics Vol. 70 (Springer, Berlin, 1974).